"Let's Agree to Disagree": Investigating the Disagreement Problem in Explainable AI for Text Summarization

Seema Aswani¹ and Sujala D. Shetty^{2*}

^{1,2*}Department of Computer Science, BITS Pilani, Dubai Campus, Academic City, Dubai, U.A.E.

*Corresponding author(s). E-mail(s): sujala@dubai.bits-pilani.ac.in; Contributing authors: p20210908@dubai.bits-pilani.ac.in;

Abstract

Explainable Artificial Intelligence (XAI) methods in text summarization are essential for understanding the model behavior and fostering trust in modelgenerated summaries. Despite the effectiveness of XAI methods, recent studies have highlighted a key challenge in this area known as the "disagreement problem". This problem occurs when different XAI methods yield conflicting explanations for the same model outcome. Such discrepancies raise concerns about the consistency of explanations and reduce confidence in model interpretations, which is crucial for secure and accountable AI applications. This work is among the first to empirically investigate the disagreement problem in text summarization, demonstrating that such discrepancies are widespread in state-of-the-art summarization models. To address this gap, we propose Regional Explainable AI (RXAI) a novel segmentation-based approach, where each article is divided into smaller, coherent segments using sentence transformers and clustering. We use XAI methods on text segments to create localized explanations that help reduce disagreement between different XAI methods, thereby enhancing the trustworthiness of AI-generated summaries. Our results illustrate that the localized explanations are more consistent than full-text explanations. The proposed approach is validated using two benchmark summarization datasets, Extreme summarization (Xsum) and CNN/Daily Mail, indicating a substantial decrease in disagreement. Additionally, the interactive JavaScript visualization tool is developed to facilitate easy, color-coded exploration of attribution scores at the sentence level, enhancing user comprehension of model explanations.

 ${\bf Keywords:}$ Disagreement Problem, Explainable AI(XAI), Regional Explanations, Text Summarization

1 Introduction

Text summarization condenses lengthy documents into meaningful summaries by emphasizing crucial information (Widyassari et al., 2022). Due to the exponential growth of information, its applications span diverse fields such as news, clinical text, and legal documents summarization (Supriyono, Wibawa, Suyono, & Kurniawan, 2024). Summarization models based on the transformers architecture (Vaswani et al., 2017) have significantly advanced text summarization, resulting in fluent and contextually meaningful summaries. However, due to their black-box nature, these models have raised concerns about reliability, transparency, and biases. (Holzinger, Saranti, Molnar, Biecek, & Samek, 2020)

Explainable Artificial Intelligence (XAI) tries to solve these concerns with techniques that provide understandable explanations of a complex AI model (Saranya & Subhashini, 2023). In text summarization, the XAI methods are intended to provide transparent and interpretable explanations for why certain words/sentences were included in or excluded from the summary. This work focuses on state-of-the-art abstractive summarization models - BART (Lewis et al., 2020) and PEGASUS (Zhang, Zhao, Saleh, & Liu, 2020), fine-tuned on the XSum and CNN/Daily Mail datasets, respectively. These datasets present complementary challenges, with XSum providing single-sentence and CNN/Daily Mail providing multi-sentence summaries.

Despite the effectiveness of XAI methods, they face a key challenge known as the disagreement problem, where different methods produce conflicting explanations (Krishna et al., 2024). This issue erodes trust and presents significant challenges in high-stakes domains such as healthcare, finance, and law. For instance, conflicting explanations can affect crucial decisions in fraud detection, disease diagnosis, or legal compliance, leading to security breaches or ethical failures. It is essential to address the disagreement problem not only for enhanced interpretability but also to ensure secure and trustworthy deployment of AI. While efforts have been made to quantify the disagreement in other domains, no prior work has explored potential solutions tailored specifically for text summarization models. To address and mitigate this issue we introduce a novel Regional Explainable AI (RXAI) framework which segments the articles into semantically coherent regions using Sentence Transformers (Song, Tan, Qin, Lu, & Liu, 2020) and clustering. To quantify the disagreement based on the underlying meaning of explanations we propose a semantic similarity-based metric called Semantic Alignment Score (SAS). As the final contribution, we present an open-source JavaScript-based tool that generates interactive sentence-level attribution visualization, providing insights into the contributions of input sentences to model predictions¹. Following are the main Research Questions(RQ) that we aim to address in this study.

- **RQ1**: To what extent do different XAI methods agree when applied to text summarization models?
- **RQ2**: How do dataset characteristics such as the input article length and summary type affect the disagreement among XAI methods in text summarization?
- **RQ3**: Does the proposed RXAI framework, through text segmentation reduce disagreement between XAI methods in text summarization?

 $^{^{1}} Access \ the \ tool \ here: \ https://github.com/SVC04/Explainable-Summarization$

In summary, the following are the key contributions of our research:

- 1. This paper offers a novel empirical analysis of the disagreement problem among different XAI methods applied to text summarization models, utilizing both predefined metrics and the proposed semantic similarity-based metric.
- 2. We propose RXAI, a novel framework that leverages segmentation-based explanations using sentence embeddings and k-means clustering to mitigate the disagreement problem.
- 3. We have developed an open-source interactive JavaScript visualization tool to analyze sentence-wise attribution scores for text summarization models.

2 Related Work

2.1 XAI Methods and Attribution Generation Framework

XAI methods have gained popularity for interpreting complex deep-learning models. In text summarization, XAI methods like LIME (Ribeiro, Singh, & Guestrin, 2016), Gradient SHAP (Lundberg & Lee, 2017), attention mechanism (Bahdanau, 2014), and DeepLIFT (Shrikumar, Greenside, & Kundaje, 2017) provide diverse perspectives for understanding model decisions. LIME approximates a model locally by perturbing input sentences, Gradient SHAP approximates Shapely values using gradient-based expectations, attention mechanism helps transformer models focus on relevant parts of the input text, while DeepLIFT assigns attribution scores by comparing each neuron's activation to a reference activation. Appendix B contains a detailed description of these methods.

Transformer-based models applied for text generation tasks require specialized tools for attribution generation. The Inseq library Sarti, Feldhus, Sickert, and van der Wal (2023) built on Captum Kokhlikyan et al. (2020), supports standard XAI methods for token and sentence-level attribution generation and an interactive heatmap visualization that enhances the interpretability of the seq2seq model prediction.

2.2 The Disagreement Problem and Its Evaluation

The disagreement problem in XAI occurs when different methods give divergent explanations for the same input for feature importance, ranking, or directional influence (Krishna et al., 2024). Prior research has made significant progress in validating the interpretability using ROAR (Remove and Retain) (Hooker, Erhan, jan Kindermans, & Kim, 2018). It has also focused on evaluating discrepancies in explanation quality with an emphasis on fidelity, stability, consistency, and sparsity (Dai, Upadhyay, Aivodji, Bach, & Lakkaraju, 2022), as well as benchmarking feature attribution techniques with synthetic datasets (Liu, Khandagale, White, & Neiswanger, 2021). However, the crucial task of assessing the inconsistency in explanations is understudied. Krishna et al. (2024) points out that most of the XAI methods differ in explanations and emphasize the need for systematic approaches to address them.

Previous studies have examined various disagreement metrics. Neely, Schouten, Bleeker, and Lucic (2022) discovered low correlations between XAI methods, questioning the validity of agreement-based evaluations. Roy et al. (2022) suggested an

aggregated approach to reduce disagreement between LIME and SHAP through prioritizing shared features. These results highlight the need for consistent metrics to evaluate and control XAI disagreement.

2.3 Proposed Solutions for Disagreement in XAI

Recent studies have proposed promising solutions to tackle the disagreement problem such as the AGREE framework Pirie, Wiratunga, Wijekoon, and Moreno-Garcia (2023) and the application of FD-Trees Laberge, Batiste Pequignot, Marchand, and Khomh (2024). The FD trees execute localized feature interactions while the AGREE framework mitigates the problem through the use of alignment-based metrics. These frameworks highlight the potential of alignment-based strategies and the potential of segmentation in tackling disagreement problem.

This work addresses the disagreement problem in text summarization by extending previous research. Building on local explanations (Laberge et al., 2024) and different agreement measurement strategies, we present the RXAI framework as a novel tool to improve the consistency of explanations between XAI methods.

3 Methodology

3.1 Phase A: Disagreement Analysis

This work follows a two-phase approach to measure and reduce disagreement between XAI methods. Phase A measures global disagreement on complete articles over two benchmark summarization datasets—XSum and CNN/Daily Mail. The system architecture of Phase A is illustrated in Fig. 1a. We examined 11 separate random batches of 500 articles each (5500 total per dataset) to ensure robustness, reduce sampling bias, and assess statistical consistency between runs. This batched setup enhances reliability and facilitates Phase B, where analysis for each batch guarantees computational feasibility while maintaining generalizability. Appendix A contains detailed statistics of both datasets.

The input articles were tokenized to a maximum length of 1,024 tokens, utilizing the Hugging Face implementation (Wolf et al., 2020). As shown in Fig. 1a the input articles were preprocessed and summarized using two state-of-the-art pre-trained models: BART (Lewis et al., 2020) fine-tuned on the XSum dataset, and PEGASUS (Zhang et al., 2020), fine-tuned on CNN/Daily Mail without additional fine-tuning. We employed four diverse XAI methods: attention (model-intrinsic), DeepLIFT (activation and backpropagation-based), LIME (perturbation-based), and Gradient SHAP (gradient-based) to generate attribution at token and sentence level. Each XAI method uses different input configurations and explanation strategies, allowing a comprehensive analysis. To quantify agreement between these attributions, both the predefined metrics proposed by Krishna et al. (2024) and proposed semantic similarity-based metrics were utilized. To represent the resulting pairwise agreement scores we have used heatmaps and some other form of visualizations.

3.2 Phase B: Tackling Disagreement through RXAI

Phase B discusses the proposed RXAI framework, which segments input text into semantically coherent regions using Sentence Transformers (Song et al., 2020) and k-means clustering method (Hartigan & Wong, 1979). The segmentation helps to analyze the disagreement problem at segment level, article level, and across all articles. By focusing on regional explanations, the RXAI framework complements the full-text disagreement analysis performed in Phase A and offers insights into the impact of explanation consistency at the segment level. Fig. 1b outlines the RXAI system architecture.

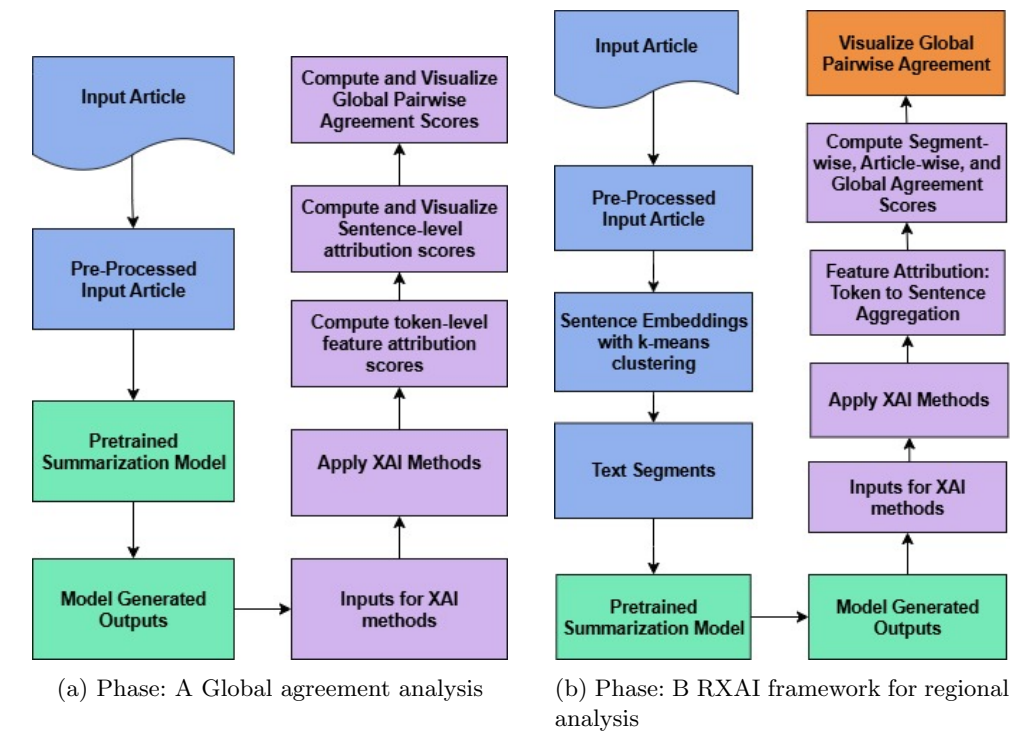


Fig. 1: System architectures for analyzing and addressing the disagreement problem in XAI methods. (a) Phase A performs global agreement analysis. (b) Phase B applies RXAI for regional evaluation. These phases can be executed in parallel, enabling a transition from a global to a more fine-grained analysis for improved explanation consistency.

3.3 Customized Pre-processing steps

Customized pre-processing steps were applied to the input articles to ensure precise detection of sentence boundaries, a critical factor for aggregating token-level attribution scores into sentence-level attribution. Periods are considered as indicators of

sentence ending. The precise identification of sentence boundaries facilitates the calculation of sentence-wise attribution scores, in contrast to previous studies that focused on token-level attributions. Following is the list of pre-processing steps applied:

- Adjusting Sentence Boundaries and Punctuation: This step is added to
 ensure proper sentence endings by correcting misplaced periods near quotation
 marks, inserting missing periods, and standardizing punctuation such as question
 marks paired with periods.
- Reducing Redundant Periods: To avoid confusion in token aggregation multiple consecutive periods are replaced with a single period in this step.
- Handling Non-Standard Period Usages: In this step, the periods in initials, URLs, email addresses, and decimal numbers are replaced with special tokens ([NAME_PERIOD_TOKEN], [WEB_PERIOD_TOKEN], [EMAIL_PERIOD_TOKEN], [NUMBER_PERIOD_TOKEN]) to avoid errors in boundary detection.

3.4 Attribution Computation and Interactive Visualization

The four XAI methods: LIME, Gradient SHAP, Attention, and DeepLIFT were implemented using Inseq library to explain the results of text summarization models. The Inseq library generates attribution scores token-wise using model.attribute() function. These token-wise scores are aggregated into sentence-wise scores using the aggregate() function. The attribution scores are normalized within the range of [0,1], ensuring consistency and comparability among attribution scores derived from several XAI methods.

To facilitate visual understanding of the link between the input text and the model-generated summary based on the generated attribution scores, we developed an interactive JavaScript-based tool. The tool accepts three inputs: Input Text Sentences, sentence-wise attribution score, and model-generated summary. Sentences are derived from the truncated input article, which is tokenized and shortened to the model's maximum token limit. The <code>inseq</code> library provides normalized token-level attribution scores, aggregated into sentence-level. However, the scale of the score differs across XAI methods. To ensure consistency and enable comparability across methods, an additional normalization step is applied to standardize the scores by applying the formula below:

$$\label{eq:score} \mbox{Normalized Score} = \frac{\mbox{Score} - \mbox{Min}}{\mbox{Max} - \mbox{Min}}$$

Upon receiving these inputs, the tool generates a color-coded plot where each sentence is assigned a color gradient (light blue to dark blue) based on its attribution score, with darker shades indicating higher importance. The tool offers an interactive hover functionality that allows users to view exact attribution scores for each sentence, enhancing transparency. For a detailed view of the tool's user interface, refer to Fig. E16 in the Appendix.

Fig. 2 presents the resulting visualization, which highlights the contributions at the sentence level to the generated summary with the help of DeepLIFT XAI method. The visualization tool provides an effective way to compare the attribution of input sentences to the generated summary, aiding in enhanced interpretability.

Explanation using Deeplift based attribution

Model Generated Summary: There is a desperate need for housing for ex-prisoners in Wales, a charity has said

Input Text:

Prison Link Cymru had 1,099 referrals in 2015-16 and said some ex-offenders were living rough for up to a year before finding suitable accommodation. V Attention Weight: 0.8365 m investment in housing would be cheaper than jailing homeless repeat offenders. The Weish Government said more people than ever were getting help to address housing problems. Changes to the Housing Act in Wales, introduced in 2015, removed the right for prison leavers to be given priority fo accommodation. Prison Link Cymru, which helps people find accommodation after their release said things were generally good for women because issues such as children or domestic violence were now considered. However, the same could not be said for men, the charity said, because issues which often affect them, such as post traumatic stress disorder or drug dependency, were often viewed as less of a priority. Andrew Stevens, who works in Welsh prisons trying to secure housing for prison leavers, said the need for accommodation was "chronic". "There's a desperate need for it, finding suitable accommodation for those leaving prison there is just a lack of it everywhere," he said. "It could take six months to a year, without a lot of help they could be on the streets for six months. "When you think of the consequences of either being on the street, especially with the cold weather at the moment or you may have a roof over your head. sometimes there is only one choice". Mr Stevens believes building more one-bedroom flats could help ease the problem. "The average price is a hundred pounds a week to keep someone in a rented flat, prison is a lot more than that so I would imagine it would save the public purse quite a few pounds," he said. Official figures show 830 one-bedroom properties were built in the year to March 2016, of an overall total of 6,900 new properties in Wales. Marc, 50, who has been in and

Fig. 2: The text plot of the attribution weights assigned over the input sentences using DeepLIFT. Normalized attribution scores are represented using color coding, where darker-colored sentences represent higher attribution weights, signifying the greater contribution to the resultant summary.

3.5 Quantifying Disagreement between XAI methods

We employed existing metrics proposed by Krishna et al. (2024) to evaluate the explanation agreement. These metrics quantify agreement at several levels. For the comparison of explanations between XAI methods, we apply four existing metrics: Feature Agreement, Rank Agreements, Spearman Rank Correlation, and Pairwise Rank Agreement (PRA) (Krishna et al., 2024). Additionally, we introduce a novel semantic similarity-based metric SAS that quantifies disagreement at the semantic level by comparing attribution-weighted sentence embeddings using cosine similarity. These metrics measure agreement based on the most significant (top-k) and relative feature ranking. Appendix C provides specific details on these measures. The selection of top-k values is inspired by Krishna et al. (2024) and adjusted to account for structural differences in the analysis. For global disagreement analysis we select $k \in [2, 10]$, which covers 25-50% of content in documents averaging 20-40 sentences. For RXAI we choose $k \in [2, 4]$ which covers 44-66% of shorter segments averaging 6-9 sentences.

The Algorithm 1 outlines the steps of computing global agreement scores for text summarization datasets. For each XAI method the attribution scores are derived, followed by pairwise top-k and relative ranking agreement computations. The pairwise agreement scores of all the articles are aggregated to achieve global agreement scores. These scores were then analyzed using different visualizations.

Algorithm 1 Compute top-k and Relative Ranking Agreement

```
1: Input: sample_news_articles, methods = [attention, deeplift, lime, gradient_shap]
2: Output: Pairwise agreement scores based on top-k and relative rankings
3: Preprocess sample_news_articles and store it in preprocessed_articles
4: Initialize qlobal\_results \leftarrow []
   for each article in preprocessed_articles do
       for each method in methods do
          Load model instance with method
7.
          out \leftarrow model\_instance.attribute(article)
8:
          Aggregate sentence spans from out and assign to qlobal_results
9.
10:
      end for
11: end for
12: for each (method1, method2) pair in methods do
       for k = 2 to 11 do
13:
          Compute and store average top-k agreement
14:
       end for
15:
       Compute and store:
16:
   (a) Average Spearman Correlation
   (b) Average Pairwise Rank Agreement
17: end for
18: Generate correlation matrices and visualizations of agreement
```

3.6 RXAI: Tackling the Disagreement Problem

To tackle the disagreement problem among XAI methods we employed the RXAI approach, hypothesizing that segmenting the input article into semantically coherent segments would reduce the level of disagreement between explanations. Algorithm 2 outlines the RXAI framework. First, the input articles are pre-processed and truncated into 1024 tokens to match the input length handled by pre-trained transformer models. Due to the high accuracy, all-mpnet-base-v2 sentence transformer (Song et al., 2020) is utilized to transform input sentences into high-dimensional embeddings followed by applying k-means clustering (Hartigan & Wong, 1979) for segmentation. The value of optimal-k is determined by maximizing the Silhouette Score (Rousseeuw, 1987) on a range $k \in [2, \min(10, \text{num_sentences} - 1)]$, to ensure clustering quality and preserving over segmentation. In cases where multiple k-values yield the same maximum silhouette score we applied a tie-breaking strategy that chooses smallest kvalue. The rationale behind this choice is: (i) computational efficiency, since a smaller number of clusters decreases the overhead of segment-level attribution; and (ii) semantic coherence, since larger segments maintain contextual flow better, which enhances explanation reliability. The clusters with fewer than two sentences are merged with the most similar cluster using cosine similarity. The k-values across articles were averaged for uniformity. Segment-level attribution scores are computed for each XAI method. These scores at segment level are aggregated into article-level disagreement scores and visualized through pairwise heatmaps for both segment and article-level analysis.

k-means was chosen for its balance between segmentation quality and computational feasibility. While DBSCAN (Ester, Kriegel, Sander, & Xu, 1996) can deal

with arbitrarily shaped clusters, it does not work well with high-dimensional sentence embeddings and needs careful fine-tuning of the ϵ parameter. In contrast, k-means offers more control over the number of clusters (k). Agglomerative clustering (Müllner, 2011) effectively captures hierarchical relationships, but it was not employed due to its high computational complexity, making it challenging to cluster the high-dimensional sentence embeddings.

Algorithm 2 Regional Explanations and Agreement Calculation

- 1: Input: $sample_news_articles$, $methods = [attention, deeplift, lime, gradient_shap]$
- 2: Output: Average agreement scores and visualizations
- 3: Preprocess and tokenize sample_news_articles into preprocessed_articles (truncate to 1024 tokens)
- 4: Encode sentences and determine optimal k for k-means clustering
- 5: Compute average k for uniform segmentation
- 6: **for** each *article* in *preprocessed_articles* **do**
- 7: Segment article using K-means with average k
- 8: Merge small clusters (fewer than two sentences) into the most similar cluster
- 9: Store segmented article in preprocessed_segments
- 10: end for
- 11: \mathbf{for} each $segmented_article$ in $preprocessed_segments$ \mathbf{do}
- 12: **for** each *method* in *methods* **do**
- 13: Compute attribution scores for each segment using the XAI method
- 14: end for
- 15: Aggregate segment-level scores into article-level disagreement
- 16: end for
- 17: Compute average disagreement scores across all articles
- 18: Generate pairwise agreement heatmaps and visualizations

4 Results

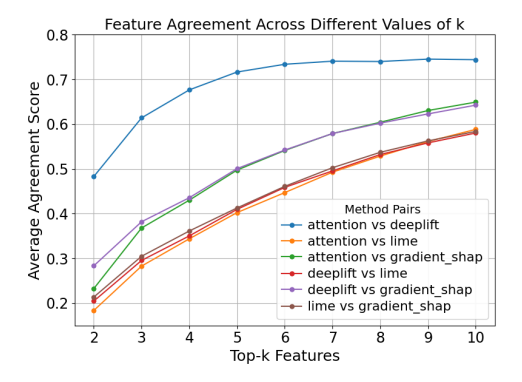
4.1 Disagreement Analysis Across XAI Methods

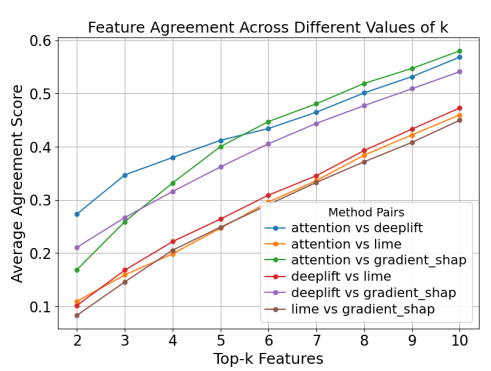
The results section is divided based on three main research questions this study has focused on. The disagreement analysis is conducted on Xsum and CNN/DM datasets using metrics discussed in appendix C. The results are evaluated on a total of 5,500 test samples from each dataset, examined across 11 random batches to ensure statistically robust results and computational feasibility for attribution generation for global and RXAI analysis. To assess the consistency and mean difference of agreement scores across all batches, we used one-way ANOVA for each method pair and k-value separately. The results of ANOVA revealed highly consistent results across the agreement metrics Feature, Rank, Semantic, and Rank Correlation agreement for Xsum (with p-value higher than 0.05) and moderate batch sensitivity for CNN/DM. Refer to Section: D.3.3 for detailed results. While the entire study covers all 11 batches, this section provides detailed results and visualizations based on a single representative batch of 500 articles. This section presents the analysis of the degree of disagreement

between XAI methods (RQ1) and assesses the influence of dataset characteristics on disagreement (RQ2).

4.1.1 RQ1.To what extent do different XAI methods agree when applied to text summarization models?

1. Feature Agreement Analysis: The feature agreement across both datasets is illustrated in Fig. 3. attention vs. DeepLIFT consistently shows the highest feature agreement for the Xsum dataset, which indicates that the two methods mostly highlight the same top features. For the CNN/DM dataset attention vs DeepLIFT exhibited the highest agreement up to k=5. However, for k>5 the attention vs Gradient SHAP surpasses attention vs. DeepLIFT, indicating that the attribution assigned by Gradient SHAP aligns more closely with attention-based explanations when considering a larger set of features. The LIME-based method pairs exhibited lowest agreement scores. The feature agreement value increases as k increases. Variability analysis of feature agreement scores is depicted in Fig. D1 in Appendix.

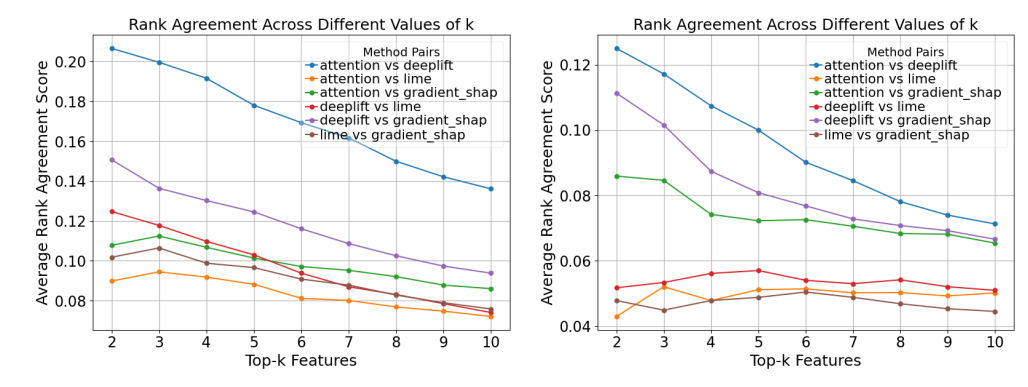




- (a) Feature agreement across different k-values for Xsum.
- (b) Feature agreement across different k-values for CNN/DM.

Fig. 3: Average feature agreement scores across top-k (k=2 to 10) features for Xsum (Fig. 3a) and CNN/DM (Fig. 3b)datasets. Feature agreement scores increase as the value of k increases. For both the datasets mostly the attention vs. DeepLIFT exhibits the highest feature agreement. Feature agreement values for the CNN/DM dataset are slightly low in magnitude compared to Xsum feature agreement scores.

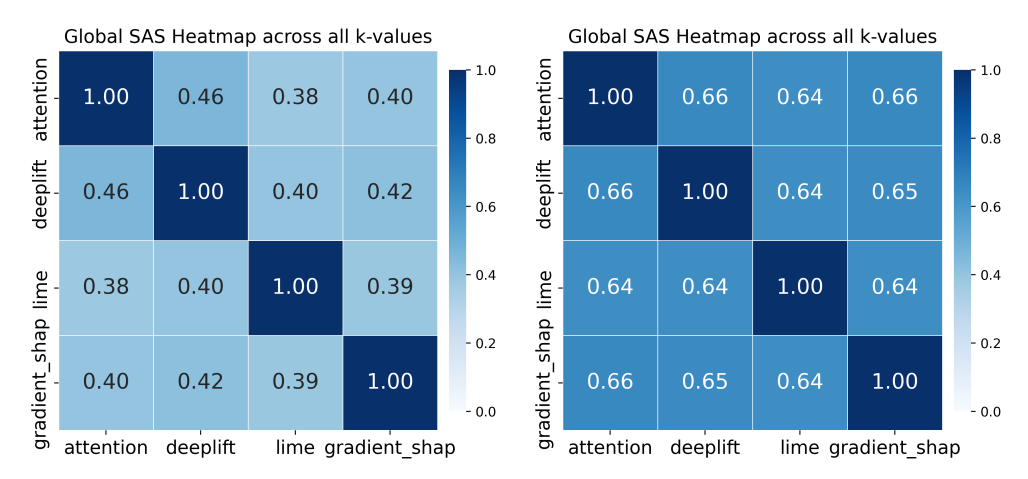
2. Rank Agreement Analysis: The rank agreement scores in Fig. 4 highlights that attention vs. DeepLIFT gives the highest rank agreement score, while the overall value of agreement is relatively low for both datasets. For all method pairs, rank agreement decreases consistently as the value of k increases. This indicates that, with more features taken into consideration, the methods disagree not only in which features they highlight but also in how they rank them. Fig. D2 in appendix D illustrates the variability of rank agreement scores across all method pairs.



(a) Rank agreement across different k-values (b) Rank agreement across different k-values for Xsum. (b) Rank agreement across different k-values for CNN/DM.

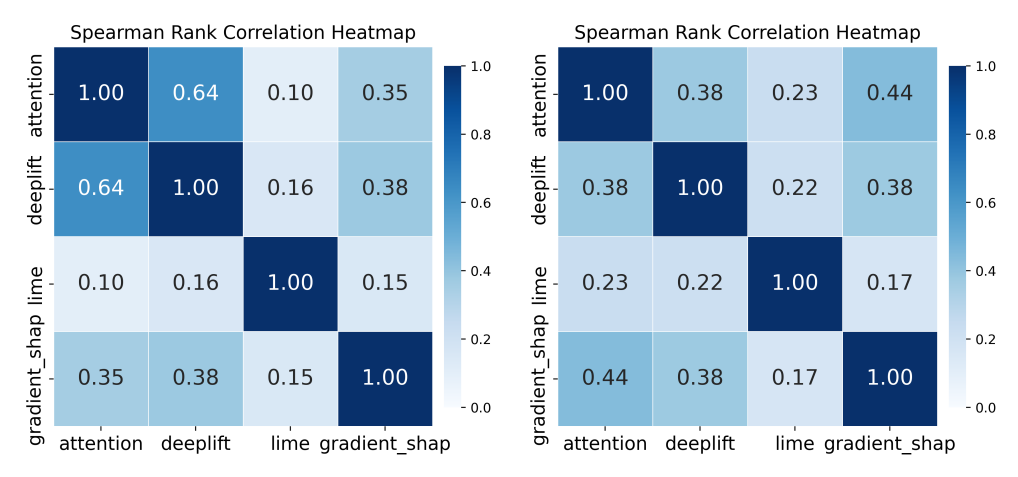
Fig. 4: Average rank agreement scores across top-k (k=2 to 10) features for Xsum (Fig. 4b) and CNN/DM (Fig. 4a) datasets. Rank agreement scores decrease as the value of k increases. For both the datasets the attention vs. DeepLIFT method pair exhibits the highest rank agreement with relatively low value. Rank agreement values for CNN/DM dataset are low in magnitude compared to Xsum rank agreement scores.

- 3. Semantic Alignment Score Analysis: The SAS scores illustrated in Fig. 5a and 5b were averaged across all k values due to their consistency, with relatively same scores across all method pairs. The semantic alignment is higher in the CNN/DM (0.64–0.66) compared to XSum (0.38–0.46), indicating stronger agreement between XAI methods in CNN/DM. This may be attributed to its discourse structure and less abstractive summary. SAS analysis per k is added in Tables: D2 and D3.
- 4. Rank Correlation Analysis: We have also applied agreement metrics based on the relative ranking of features to quantify disagreement further. Fig. 6 presents the average rank correlation heatmaps. In the Xsum dataset, the attention vs. DeepLIFT method pair consistently exhibited high agreement, with a high average correlation value. In contrast, for the CNN/DM dataset attention vs. Gradient SHAP has achieved the highest correlation value. However, the average correlation value is relatively low. Across both datasets, all other method pairs display significantly lower rank correlation scores, highlighting a strong disagreement in relative ranking of features among these methods. The results of pairwise rank agreement metric are discussed in appendix D in Fig. D3.



- (a) Average SAS across all k values for XSum Dataset
- (b) Average SAS across all k values for CNN/DM Dataset

Fig. 5: Semantic Alignment heatmaps showing average SAS agreement between explanation methods on both datasets. Higher scores indicate stronger semantic alignment.



- (a) Rank correlation heatmap for Xsum.
- (b) Rank correlation heatmap for CNN/DM.

Fig. 6: Average spearman rank correlation heatmap for Xsum (Fig. 6a) and CNN/DM (Fig. 6b) datasets. Overall agreement scores based on rank correlation are low, indicating significant disagreement between XAI methods for both Xsum and CNN/DM datasets.

4.1.2 RQ2. How do dataset characteristics such as the input article length and summary type affect the disagreement among XAI methods in text summarization?

Based on the empirical analysis presented in section 4.1.1, the global agreement scores reveal significant disagreement among XAI methods across both datasets, Xsum and CNN/DM. The diversity of document length and summary type between datasets impacts the disagreement scores. The average length of the documents in XSum dataset is shorter than CNN/DM as discussed in Table: A1. The Xsum highlights a single-sentence summary whereas CNN/DM consists multi-sentence summary. As a result, the disagreement scores of CNN/DM are lower than those in XSum. This highlights the challenges of handling longer lengths of input articles and summaries. However this trend is reversed for semantic alignment (SAS) where CNN/DM exhibits higher semantic alignment compared to Xsum, likely due to its structure and less abstractive summary. Despite the differences in the magnitude of disagreement scores, the trend of disagreement remains consistent across both datasets. This indicates that the disagreement observed has not occurred randomly and the dataset characteristics play a key role in the disagreement analysis.

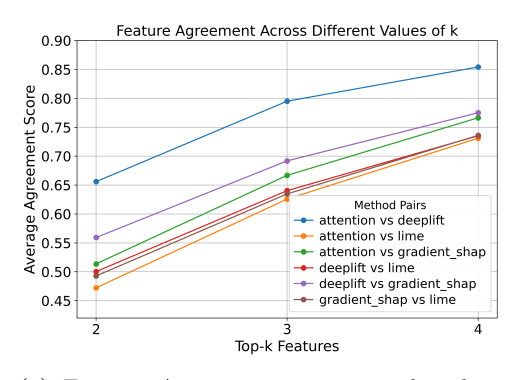
Key takeaways: From our empirical analysis, it is evident that the XAI methods disagree significantly when applied to text summarization. The attention vs. DeepLIFT method pair frequently shows the highest agreement, indicating consistent explanations in contrast, LIME tends to diverge significantly from other methods and display consistently lower agreement scores. The diversity of documents in terms of length and summary types affects the overall magnitude of disagreement scores, resulting in higher magnitude of agreement scores for Xsum dataset with comparatively smaller documents than CNN/DM dataset, whereas the Semantic Alignment Scores exhibit opposite trend, with CNN/DM dataset having higher alignment scores.

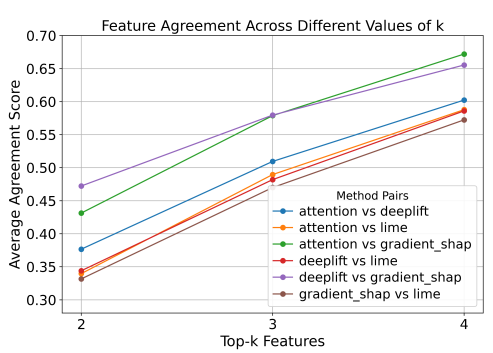
4.2 RQ3. Does the proposed RXAI framework, through text segmentation, reduce disagreement between XAI methods in text summarization?

1. Feature Agreement Analysis: The feature agreement analysis of top-k features for segmented articles is shown in Fig. 7. The attention vs. DeepLIFT pair in XSum dataset (Fig. 7a) obtains the highest feature agreement score of roughly 0.85 for k=4, suggesting that it is highly aligned following text segmentation. In the CNN/DM dataset (Fig: 7b), method pairs that include Gradient SHAP demonstrate the most significant enhancement, with attention vs Gradient SHAP and DeepLIFT vs. Gradient SHAP attaining highest feature agreement scores of 0.67 and 0.66, respectively for k=4. These outcomes demonstrate the effectiveness of RXAI framework. In both datasets. LIME-based method pairs continue to exhibit the lowest agreement. However, agreement scores of LIME-based method pairs have significantly improved.

To compare and verify the effectiveness of RXAI framework appendix Figures: D4 of Xsum and D5 of CNN/DM dataset present global vs. regional feature

agreement heatmaps at k=4. The heatmaps of both datasets highlight significant improvement in feature agreement scores compared to global feature agreement. To test the significant mean difference of agreement scores between global and segmented articles, we have used Wilcoxon signed rank test for all method pairs across different k-values. This non-parametric test was chosen because it does not assume normality and is well-suited for paired comparison between global and regional scores. For both datasets the p-values were below 0.05, highlighting significant mean difference. Appendix Tables D9 and D10 report the p-values across different k-values and method pairs, based on the same representative batch of 500 articles used in the main analysis.



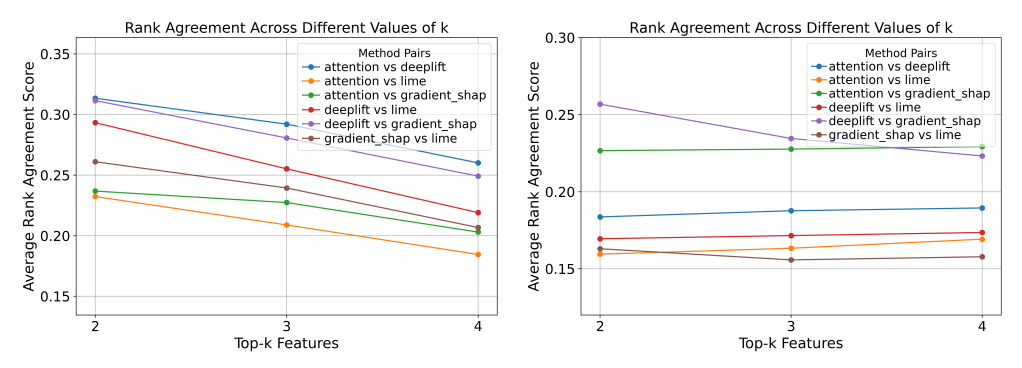


- (a) Feature Agreement across top-k values (Segmented Articles) for Xsum dataset.
- (b) Feature Agreement across top-k values (Segmented Articles) for CNN/DM dataset.

Fig. 7: Average feature agreement scores for segmented articles of Xsum (Fig. 7a) and CNN/DM (Fig. 7b). The line plot highlights significant improvements in agreement, with the attention vs. DeepLIFT pair achieving the highest score for Xsum and attention vs. Gradient SHAP for CNN/DM.

2. Rank Agreement Analysis: The regional rank agreement plot of the Xsum dataset in Fig. 8a shows increased and relatively stable rank agreement scores across the different values of k, with DeepLIFT vs. Gradient SHAP achieving the highest rank agreement of approximately 0.32 for k = 4 compared to the global score of 0.13, indicating improved agreement scores after segmentation. The LIME-based method pairs also achieve improved rank agreement scores after segmentation with DeepLIFT vs. LIME achieving the highest rank agreement of 0.28 at k = 4 compared to a global agreement score of 0.11. The rank agreement plot of the CNN/DM shown in Fig. 8b highlights a similar trend as Xsum dataset with attention vs. Gradient SHAP and DeepLIFT vs. Gradient SHAP having the highest agreement. The segmentation approach does improve the rank agreement scores.

The Analysis of Rank correlation and SAS revealed that the agreement scores based on rank correlation and SAS scores remain largely consistent as the global agreement scores. The graphs are added in the Appendix D.2.



- (a) Rank Agreement across top-k values (Segmented Articles) for Xsum dataset.
- (b) Rank Agreement across top-k values (Segmented Articles) for CNN/DM.

Fig. 8: Average rank agreement scores across top-k values for segmented articles of Xsum (Fig. 8a) and CNN/DM dataset (Fig. 8b). The plots demonstrate overall improvement in rank agreement scores for both datasets text segmentation.

Key takeaways: The results of RXAI based on top-k features on both datasets highlight that while the overall agreement improves between XAI methods, the extent of this improvement varies between different agreement metrics. Feature agreement and rank agreement are significantly enhanced, but rank agreement metrics reveal a continued disagreement. SAS scores remain relatively unchanged after applying RXAI approach. On the contrary, relative ranking-based approaches do not exhibit improved agreement scores on both datasets. Overall, the results based on syntactic top-k feature metrics highlight that regional explanations increase the agreement level with statistically significant differences in mean scores, validating the hypothesis that text segmentation improves the consistency of explanations across methods.

5 Discussion

5.1 Disagreement Problem among XAI methods

Our results confirm significant disagreement among XAI methods in text summarization. Model-specific methods, such as attention vs. DeepLIFT consistently demonstrate higher agreement, reflecting their focus on global attributions, while model-agnostic method like LIME shows lower agreement due to their perturbation-based approach.

The disagreement problem is critical in high-stake and secure AI applications. In healthcare, inconsistency of explanations may lead to conflicting diagnoses. In legal and financial domains, conflicting explanations can mislead contractual interpretations or risk assessments. One potential future direction would be to use Large Language Models (LLMs) as mediators to aggregate explanations of different XAI methods into more

consistent explanations. Additionally, conversational AI agents could enhance interpretability by enabling interactive investigation of attribution discrepancies, helping users understand why disagreements occur.

5.2 Impact of RXAI framework

Silhouette-based k-means segmentation mitigates the disagreement problem. Our findings demonstrate that segmentation serves as a promising strategy to mitigate this problem, while also revealing that the impact of segmentation varies across different agreement metrics. The proposed approach of utilizing silhouette-based clustering in high-dimensional context has known limitations (as discussed in 5.3). Future work should explore alternate clustering validation indices or adapt dimensionality reduction techniques to address this limitation. Applying RXAI framework introduces computational overhead. The segmented articles of Xsum dataset requires 39 hours of computation compared to 29 hours of global analysis (34% increase). For CNN/DM, it requires 78.6 hours of computation compared to 53.9 hours of global computation (45.7% increase) for a 500 article batch. In case of LIME, which is particularly compute-intensive due to the lack of batched attribution support in the Inseq library, attribution generation for segmented data of 500 articles based on LIME required 29 hours for XSum and approximately 65 hours for CNN/DM—accounting for over 74% and 80% of the total execution time, respectively. The computational overhead stems from segmentation, XAI method execution (with LIME being primary contributor) on segments, and the number of articles to process. This results in $O(n \times s \times m)$ complexity where s, n, and m represent segment, method, and number of articles. This computational cost represents a reasonable trade-off for applications requiring highly consistent explanations, though it limits its deployment in time-sensitive scenarios. Future work should explore efficient segmentation approaches and optimization techniques.

While RXAI effectively enhances agreement between explanations it may introduce semantic or coherence drift between input article and segments, leading to diverging segments that may not fully preserve the original context. To evaluate this we measured semantic similarity and coherence between input articles and segments. The results illustrate high semantic similarity more than 90% between input article and segments for both datasets (refer Table D11), ensuring semantic preservation. Additionally, the coherence analysis reveals minor drift between article and its segmented version, suggesting that overall coherence is largely maintained with moderate drift (refer Table D12). RXAI can be extended beyond news summarization with its careful adoption of domain-specific requirements and structured segmentation strategies in fields such as healthcare, legal, and financial text summarization. Future work could explore topic-aware segmentation and graph-based clustering to enhance scalability while preserving meaning and coherence when applying the RXAI approach.

5.3 Limitations

1. This study demonstrates the existence of XAI disagreement in text summarization. However, it does not investigate the root cause of why these methods disagree. Future research could explore the root cause of disagreement among XAI methods.

- 2. Although silhouette score is widely used metric for identifying optimal number of clusters, its reliability in high-dimensional embedding spaces is affected by the curse of dimensionality. This may weaken the distinction between intra-cluster and inter-cluster distances, making it challenging to detect true cluster boundaries.
- 3. In this study, we have utilized English-language news summarization datasets as a foundational evaluation of RXAI in general news context. However, we acknowledge that adapting RXAI framework in summarization tasks such as legal, clinical or scientific text summarization may pose challenges due to longer input sequences, specialized terminologies and domain-specific structural complexity.
- 4. We have tested explanation disagreement and RXAI framework on two encoder-decoder transformer model, BART and PEGASUS. While these models are strong baselines, they share similar architecture. The effectiveness of RXAI framework to other model types such as LED, T5, or decoder-only models like GPT and LLaMA, is untested and calls for future work.

5.4 Future Work

For future work, we will investigate the performance of XAI methods in various text summarization domains such as health, finance, and legal. We will study the impact of domain-specific training on global and regional agreement of XAI methods. Future work could explore domain-adaptive segmentation strategies, where RXAI could be guided by domain-specific discourse markers, ontologies, or structural cues. Comparing agreement scores between models trained on domain-specific datasets and those trained on general-purpose datasets will allow researchers to determine whether specialized training affects the amount of agreement among XAI methods. Additionally, we will explore optimization strategies to improve the scalability of the RXAI approach on larger datasets. Future work should also assess a wide range of summarization models to evaluate whether the disagreement trend and RXAI effectiveness generalize across different model variants. Such evaluation will help evaluate architecture-dependent variations and ensure the effectiveness of RXAI in diverse paradigms. Finally, to assess the effectiveness of the proposed visualization tool in enhancing interpretability and user trust, future iterations could involve human-centered evaluations.

6 Conclusion

Our work generates empirical evidence of the existence of the disagreement problem in XAI for text summarization. The results indicate that, on both datasets: Xsum and CNN/DM, attention and DeepLIFT reflect higher agreement consistently, while LIME shows lower agreement with other methods because of the inherently different explanation generation approach. To mitigate this, we propose RXAI, a novel segmentation-based approach. The proposed framework effectively enhances the agreement scores, especially feature agreement, by splitting articles into semantically coherent segments. The effectiveness of the RXAI approach in generating stable explanations can enhance trust in AI-driven decisions, specifically for security-sensitive

applications. This paper contributes toward state-of-the-art improvement in the consistency and interpretability of Explainable AI for text summarization and also lays the base for further research in this direction.

References

- Bahdanau, D. (2014). Neural machine translation by jointly learning to align and translate. arXiv preprint arXiv:1409.0473,
- Dai, J., Upadhyay, S., Aivodji, U., Bach, S.H., Lakkaraju, H. (2022). Fairness via explanation quality: Evaluating disparities in the quality of post hoc explanations. *Proceedings of the 2022 aaai/acm conference on ai, ethics, and society* (p. 203–214). Association for Computing Machinery.
- Ester, M., Kriegel, H.-P., Sander, J., Xu, X. (1996). A density-based algorithm for discovering clusters in large spatial databases with noise. *Proceedings of the second international conference on knowledge discovery and data mining* (p. 226–231). AAAI Press.
- Hartigan, J.A., & Wong, M.A. (1979). Algorithm as 136: A k-means clustering algorithm. Journal of the royal statistical society. series c (applied statistics), 28(1), 100–108,
- Holzinger, A., Saranti, A., Molnar, C., Biecek, P., Samek, W. (2020). Explainable ai methods-a brief overview. *International workshop on extending explainable ai beyond deep models and classifiers* (pp. 13–38).
- Hooker, S., Erhan, D., jan Kindermans, P., Kim, B. (2018). Evaluating feature importance estimates.
- Jwalapuram, P., Joty, S., Lin, X. (2022, May). Rethinking self-supervision objectives for generalizable coherence modeling. *Proceedings of the 60th annual meeting of the association for computational linguistics (volume 1: Long papers)* (pp. 6044–6059). Association for Computational Linguistics.
- Kokhlikyan, N., Miglani, V., Martin, M., Wang, E., Alsallakh, B., Reynolds, J., ... others (2020). Captum: A unified and generic model interpretability library for pytorch. arXiv preprint arXiv:2009.07896,
- Krishna, S., Han, T., Gu, A., Wu, S., Jabbari, S., Lakkaraju, H. (2024). The disagreement problem in explainable machine learning: A practitioner's perspective. Transactions on Machine Learning Research,

- Laberge, G., Batiste Pequignot, Y., Marchand, M., Khomh, F. (2024, 02–04 May). Tackling the XAI disagreement problem with regional explanations. Proceedings of the 27th international conference on artificial intelligence and statistics (Vol. 238, pp. 2017–2025). PMLR.
- Lewis, M., Liu, Y., Goyal, N., Ghazvininejad, M., Mohamed, A., Levy, O., ... Zettlemoyer, L. (2020, July). BART: Denoising sequence-to-sequence pre-training for natural language generation, translation, and comprehension. *Proceedings of the 58th annual meeting of the association for computational linguistics* (pp. 7871–7880). Association for Computational Linguistics.
- Liu, Y., Khandagale, S., White, C., Neiswanger, W. (2021). Synthetic benchmarks for scientific research in explainable machine learning. *Proceedings of the neural information processing systems datasets and benchmarks track (neurips 2021)*.
- Lundberg, S.M., & Lee, S.-I. (2017). A unified approach to interpreting model predictions. *Proceedings of the 31st international conference on neural information processing systems* (p. 4768–4777). Red Hook, NY, USA: Curran Associates Inc.
- Müllner, D. (2011). Modern hierarchical, agglomerative clustering algorithms. arXiv preprint arXiv:1109.2378, ,
- Neely, M., Schouten, S.F., Bleeker, M., Lucic, A. (2022). A song of (dis) agreement: Evaluating the evaluation of explainable artificial intelligence in natural language processing. *Hhai2022: Augmenting human intellect* (pp. 60–78). IOS Press.
- Pirie, C., Wiratunga, N., Wijekoon, A., Moreno-Garcia, C.F. (2023). Agree: a feature attribution aggregation framework to address explainer disagreements with alignment metrics. (p. 184-199). CEUR-WS.
- Ribeiro, M.T., Singh, S., Guestrin, C. (2016). "why should i trust you?": Explaining the predictions of any classifier. *Proceedings of the 22nd acm sigkdd international conference on knowledge discovery and data mining* (p. 1135–1144). New York, NY, USA: Association for Computing Machinery.
- Rousseeuw, P.J. (1987). Silhouettes: A graphical aid to the interpretation and validation of cluster analysis. *Journal of Computational and Applied Mathematics*, 20, 53-65, https://doi.org/https://doi.org/10.1016/0377-0427(87)90125-7
- Roy, S., Laberge, G., Roy, B., Khomh, F., Nikanjam, A., Mondal, S. (2022). Why don't xai techniques agree? characterizing the disagreements between post-hoc explanations of defect predictions. 2022 ieee international conference on software maintenance and evolution (icsme) (p. 444-448).

- Saranya, A., & Subhashini, R. (2023). A systematic review of explainable artificial intelligence models and applications: Recent developments and future trends. Decision Analytics Journal, 7, 100230, https://doi.org/10.1016/j.dajour.2023.100230
- Sarti, G., Feldhus, N., Sickert, L., van der Wal, O. (2023, July). Inseq: An interpretability toolkit for sequence generation models. *Proceedings of the 61st annual meeting of the association for computational linguistics (volume 3: System demonstrations)* (pp. 421–435). Association for Computational Linguistics.
- Shrikumar, A., Greenside, P., Kundaje, A. (2017, 06–11 Aug). Learning important features through propagating activation differences. *Proceedings of the 34th international conference on machine learning* (Vol. 70, pp. 3145–3153). PMLR.
- Song, K., Tan, X., Qin, T., Lu, J., Liu, T.-Y. (2020). Mpnet: masked and permuted pre-training for language understanding. *Proceedings of the 34th international conference on neural information processing systems*. Curran Associates Inc.
- Sundararajan, M., Taly, A., Yan, Q. (2017). Axiomatic attribution for deep networks. Proceedings of the 34th international conference on machine learning - volume 70 (p. 3319–3328). JMLR.org.
- Supriyono, Wibawa, A.P., Suyono, Kurniawan, F. (2024). A survey of text summarization: Techniques, evaluation and challenges. *Natural Language Processing Journal*, 7, 100070, https://doi.org/https://doi.org/10.1016/j.nlp.2024.100070
- Vaswani, A., Shazeer, N., Parmar, N., Uszkoreit, J., Jones, L., Gomez, A.N., ... Polosukhin, I. (2017). Attention is all you need. *Proceedings of the 31st international conference on neural information processing systems* (p. 6000–6010). Red Hook, NY, USA: Curran Associates Inc.
- Widyassari, A.P., Rustad, S., Shidik, G.F., Noersasongko, E., Syukur, A., Affandy, A., Setiadi, D.R.I.M. (2022). Review of automatic text summarization techniques and methods. *Journal of King Saud University Computer and Information Sciences*, 34(4), 1029–1046, https://doi.org/10.1016/j.jksuci.2020.05.006
- Wolf, T., Debut, L., Sanh, V., Chaumond, J., Delangue, C., Moi, A., ... Rush, A. (2020, October). Transformers: State-of-the-art natural language processing. Proceedings of the 2020 conference on empirical methods in natural language processing: System demonstrations (pp. 38–45).
- Zhang, J., Zhao, Y., Saleh, M., Liu, P. (2020, 13–18 Jul). PEGASUS: Pre-training with extracted gap-sentences for abstractive summarization. *Proceedings of the 37th international conference on machine learning* (Vol. 119, pp. 11328–11339).

Appendix A Text Summarization Dataset

This study utilizes two benchmark datasets, XSum and CNN/Daily Mail, for evaluating text summarization models and their explanations. The XSum dataset comprises $\sim\!204\mathrm{K}$ training articles and $\sim\!11\mathrm{K}$ test articles, with one-sentence abstractive summaries from BBC News. CNN/Daily Mail includes $\sim\!287\mathrm{K}$ training articles and $\sim\!11\mathrm{K}$ test articles with multi-sentence extractive summaries. Random samples of 500 test articles were selected from each dataset for analysis. Table: A1 provides a comprehensive breakdown of the average statistics for both datasets.

Table A1: Comparison of Average Statistics between CNN/Daily Mail and XSum Datasets.

Statistic	CNN/Daily Mail	XSum	
Average Document Length	\sim 760 words	\sim 431 words	
Average Summary Length	$\sim 56 \text{ words}$	~ 23 words	
Type of Summaries	Extractive (highlight-	Abstractive (one-	
	based summaries)	sentence summaries)	
Domain	News articles (CNN	BBC News (various	
	and Daily Mail)	topics)	

Appendix B XAI methods

1. LIME (Local Interpretable Model-agnostic Explanations)

LIME locally approximates a complex model using an interpretable model to explain individual predictions (Ribeiro et al., 2016). LIME perturbs the input samples, observes changes, and derives an interpretable model on the sampled perturbations. In the text summarization task, LIME tries to explain the importance of a particular word or sentence by removing some of them from the input text. It also observes the effects of such changes on the generated summary. The interpretable model describes the local behavior of the original model around a given prediction. To generate the attribution, LIME minimizes the objective function stated below:

$$\xi(x) = \arg\min_{g \in G} \mathcal{L}(f, g, \pi_x) + \Omega(g)$$
(B1)

where:

- $\xi(x)$: Explanation of the input x.
- $g \in G$: A selected model g from the class of interpretable models.
- $\mathcal{L}(f, g, \pi_x)$: The fidelity loss function
- π_x : The proximity measure
- $\Omega(g)$: A complexity measure of the interpretable model g.
- f: The original complex model being explained, which maps the input space $x \in \mathbb{R}^d$ to a real number.

2. Gradient SHAP (SHapley Additive exPlanations using gradients)

Gradient SHAP provides an estimation for the accurate and efficient feature attribution, combining the SHAP values (Lundberg & Lee, 2017) and Integrated Gradients (Sundararajan, Taly, & Yan, 2017). Gradient SHAP can be applied in text summarization to assign the importance of every word or token by calculating the gradient with respect to the output for every input feature that resulted in a given summary. This method effectively points out which part of the input text contributes much to the resulting summary. It uses the following formula for the estimation of an attribution score:

Attribution =
$$\mathbb{E}_{\text{baselines}} [\text{gradients} \times (\text{inputs} - \text{baselines})]$$
 (B2)

This formula captures the expected contribution of input features to the model's prediction by averaging the gradients over multiple baselines.

3. attention

The attention mechanism introduced by (Bahdanau, 2014) is extensively applied in transformer models to concentrate on pertinent segments of the input text during output generation. The attention mechanism computes a weighted sum of the input features, where weights are calculated depending on the relevance of each feature to the output produced at a given step. Self-attention (Vaswani et al., 2017) improves this idea by allowing the model to evaluate the relevance of certain tokens over the whole input sequence. In text summarization, the attention mechanism helps the model to capture the most crucial information by allowing it to selectively focus on different parts of the input text throughout the generation of each summary word.

Attention
$$(Q, K, V) = \operatorname{softmax}\left(\frac{QK^T}{\sqrt{d_k}}\right)V$$
 (B3)

where Q (query), K (key), and V (value) are matrices derived from the input, and d_k is the dimension of the key vectors.

4. DeepLIFT (Deep Learning Important FeaTures)

(Shrikumar et al., 2017) proposed DeepLIFT, a method for assigning the prediction score of a deep learning model to its input features. The DeepLIFT method compares every neuron's activation to a reference activation. The method assigns the meaning of each word or phrase in the input text by analyzing how changes in the input affect the output summary, to provide insights into the decision-making process of the text summarization. DeepLIFT employs a "summation-to-delta" principle that is pointed out in Equation 4 below.

$$\sum_{i=1}^{n} C_{\Delta x_i \Delta o} = \Delta o, \tag{B4}$$

where (o=f(x)) is the model output, ($\Delta~o=f(x)$ - f(r)), ($\Delta~x_i=x_i$ - r_i), and r is the reference input.

Appendix C Disagreement Metrics

To quantify the degree of disagreement among various XAI methods, multiple metrics that assess various aspects of feature importance and ranking were utilized after the explanations were generated.

C.0.1 Agreement Measurement based on Top-k features

In this category of measurement following two metrics were employed to quantify the degree of agreement between two pairs of explanations based on their most important (top- k) features. The value of k initiates at 2, denoting the top-2 features, and may be extended to any k value, dependent upon the length of the articles under analysis.

1. Semantic Alignment Score (SAS)

We propose SAS, a semantic similarity-based metric to evaluate semantic alignment between different XAI methods. Unlike previously suggested measures that heavily rely on syntactic similarity, SAS employs sentence embedding to capture semantic relationships across explanations. It provides a unique perspective for measuring disagreement between XAI methods for text data. The steps to calculate SAS are listed below:

- Selection of Top-k Features: The top-k sentences for each XAI method are selected based on their attribution score.
- To convert the sentences into a dense vector space the sentence embeddings are generated for the selected top-k sentences.
- Weighting by Attribution Scores: The sentence embeddings are multiplied with their attribution score to emphasize their contribution
- Cosine Similarity Computation: Pairwise cosine similarity is computed between the weighted sentence embeddings.
- Averaging for Agreement: To derive the global SAS value across all method pairs, the average similarity across all top-k features is calculated.
 The SAS formula is defined as:

$$SAS(E_a, E_b, k) = \frac{1}{k} \sum_{i=1}^{k} cos_sim(S_{E_a, i} \cdot Emb_{E_a, i}, S_{E_b, i} \cdot Emb_{E_b, i})$$

Where, E_a , E_b are Explanations from two methods, $S_{E_a,i}$, $S_{E_b,i}$ are Attribution scores for the *i*-th top feature, $\text{Emb}_{E_a,i}$, $\text{Emb}_{E_b,i}$ are Sentence embeddings for the *i*-th top feature and k is Number of top features.

2. Feature Agreement

Feature agreement was the first metric applied in this study, and it referred to the degree to which two explanations agree on their most important features. It calculates the ratio of the number of common features between the two top-k feature sets from both explanations.

Mathematically, it is defined as:

Feature Agreement
$$(E_a, E_b, k) = \frac{|\text{TF}(E_a, k) \cap \text{TF}(E_b, k)|}{k}$$

where $\mathrm{TF}(E,k)$ returns the set of top-k features of explanation E based on the magnitude of feature importance values. Ea and Eb are explanations of two methods a and b.

3. Rank Agreement

The rank agreement metric compares the sets of top-k features, including their relative ordering in addition to their intersection of common features. It offers a more rigorous measure than simple feature agreement because it includes the positional ordering of features, which can greatly influence the interpretation of model explanations. The metric computes the fraction of features that are both present in the top-k feature sets of both explanations and share the same rank inside those sets, considering two explanations E_a and E_b . It can be computed using the formula below: Rank Agreement(E_a, E_b, k) =

$$\frac{|\{s \mid s \in T_a \cap T_b \wedge \operatorname{rank}(E_a, s) = \operatorname{rank}(E_b, s)\}|}{k}$$
(C5)

Here.

 $T_a = \text{top_features}(E_a, k) \text{ and } T_b = \text{top_features}(E_b, k).$

S represents the entire set of features, top_features (E,k) is the set of top-k features in explanation E, and rank (E,s) returns the rank or position of the feature s within the explanation E.

C.0.2 Agreement Measurement based on Relative ordering of features

The following two measures rely on the relative feature ordering. Two explanations are considered to be different if the relative ordering of the features of interest varies between them.

1. Rank Correlation

To quantify the agreement between the relative ordering of features in two explanations, E_a and E_b , Spearman's rank correlation coefficient is used. This metric quantifies the degree of correlation between the rankings of a selected set of features. The rank correlation between two explanations Rank Correlation(E_a, E_b, F) can be computed as:

$$r_s(\operatorname{Ranking}(E_a, F), \operatorname{Ranking}(E_b, F))$$
 (C6)

Where F is a selected set of features, r_s represents Spearman rank correlation coefficient, and Ranking(E,F) is the rank assigned to the features in F based on explanation E. Lower correlation values indicate a higher level of disagreement in the ordering of features.

2. Pairwise Rank Agreement (PRA)

It quantifies the agreement of the relative ordering of feature pairs across two explanations. This metric shows whether the relative importance of every pair of features in one explanation matches with the same pair in another. Specifically,

it evaluates the proportion of feature pairs for which the relative ranking stays constant across both models. The formula for Pairwise Rank Agreement is given below:

$$PRA(E_a, E_b, F) = \frac{\sum_{i < j} \mathbf{1}[Rank_a(f_i, f_j) = Rank_b(f_i, f_j)]}{\binom{|F|}{2}}$$
(C7)

Where $F = \{f_1, f_2, \ldots\}$ is the set of selected features, and $\mathbf{1}$ is an indicator function that returns 1 if the relative ranking of f_i and f_j is the same in both explanations and 0 otherwise. The denominator $\binom{|F|}{2}$ represents the total number of feature pairs. $\operatorname{Rank}_a(f_i, f_j)$ represents the relative ranking of features f_i and f_j in explanation E_a . $\operatorname{Rank}_b(f_i, f_j)$ represents the relative ranking of the same feature pair in explanation E_b .

Appendix D Results of Disagreement Analysis

D.1 Disagreement analysis on Full-text articles (Same Representative Batch used in Section:4.1)

• Semantic Alignment Score To measure the agreement between explanation methods based on semantic alignment, we have used the SAS metric. The Analysis of Xsum and CNN dataset across different top-k values (k = 2 to 8) is depicted in Table: D2 and Table: D3, highlighting that the semantic agreement scores across different k-values remain largely consistent. Since the SAS values are consistent across different k-values, the top-k is selected from 2 to 8. As depicted in tables D2 and D3, the semantic agreement scores for CNN/DM are higher than the scores of Xsum, diverging from the pattern observed in syntactic agreement metrics, where Xsum typically scored higher. This suggests that the higher agreement in CNN/DM may stem from its distinctive discourse structure when compared to Xsum.

Table D2: Average SAS scores across k values (2 to 8) for each XAI method pair on the XSum dataset batch presented in section 4.1.

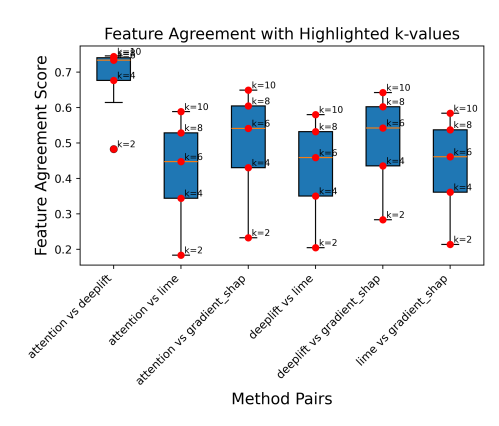
Method 1	Method 2	k=2	3	4	5	6	7	8
attention	deeplift	0.480	0.475	0.470	0.465	0.460	0.456	0.449
attention	gradient_shap	0.407	0.408	0.404	0.404	0.401	0.399	0.398
attention	lime	0.380	0.383	0.384	0.385	0.382	0.382	0.382
deeplift	gradient_shap	0.432	0.423	0.418	0.417	0.413	0.409	0.407
deeplift	lime	0.403	0.399	0.397	0.396	0.394	0.391	0.390
lime	$gradient_shap$	0.388	0.390	0.389	0.392	0.391	0.390	0.388

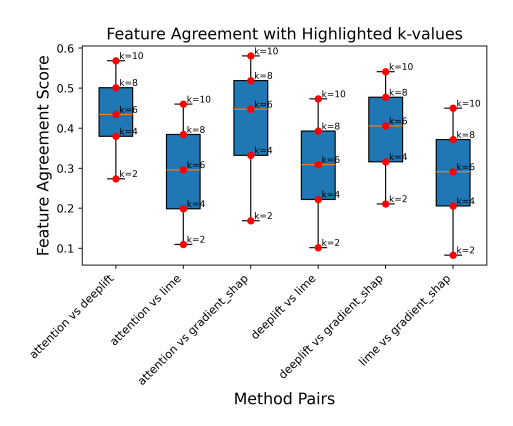
• Box Plot of Feature Agreement The Fig. D1 illustrates the variability of feature agreement scores across highlighted top-k values (k = all even numbers between 2 to 10) for both datasets. The box plot of Xsum as shown in Fig. D1a presents consistent

Table D3: Average SAS scores across k values (2 to 8) for different XAI method pairs in the CNN/DM dataset batch presented in section 4.1.

Method 1	Method 2	k=2	3	4	5	6	7	8
attention	DeepLIFT	0.660	0.661	0.662	0.662	0.662	0.660	0.659
attention	Gradient_SHAP	0.657	0.657	0.654	0.657	0.658	0.657	0.658
attention	lime	0.634	0.640	0.644	0.648	0.649	0.649	0.650
DeepLIFT	$Gradient_SHAP$	0.653	0.656	0.653	0.653	0.654	0.653	0.653
DeepLIFT	lime	0.629	0.636	0.641	0.643	0.644	0.647	0.649
lime	$Gradient_SHAP$	0.632	0.636	0.641	0.642	0.644	0.643	0.645

feature agreement scores with low variability compared to CNN/DM dataset. The box plot of the CNN/DM dataset, as shown in Fig. D1b, presents a high variability of feature agreement scores compared to Xsum, with LIME-based pairs having the highest variability across all other method pairs.

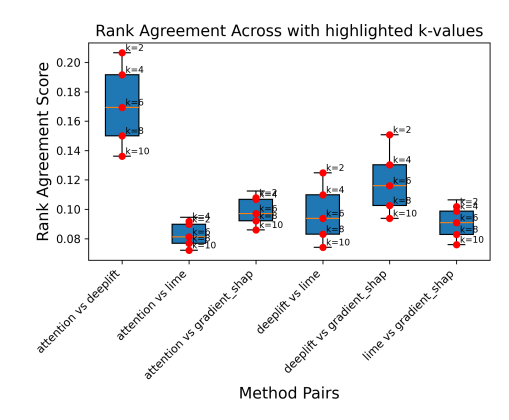


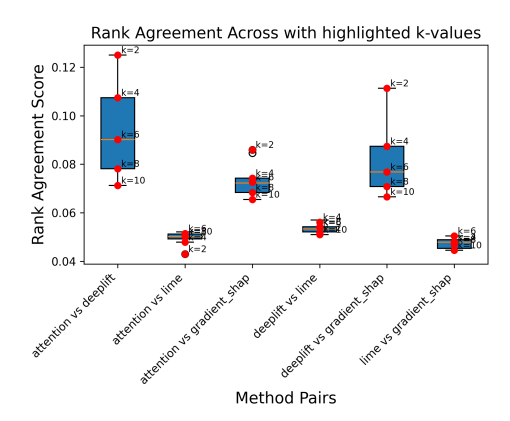


- (a) Box plot of feature agreement with highlighted k-values for Xsum.
- (b) Box plot of feature agreement with highlighted k-values for CNN/DM.

Fig. D1: Box plot of Average feature agreement scores across highlighted k-values for Xsum (Fig. D1a) and CNN/DM dataset (Fig. D1b). The box plot of the Xsum dataset indicates low variability and high feature agreement scores compared to CNN/DM, showing high variability and lower agreement scores.

• Box Plot of Rank Agreement The box plot of rank agreement scores is depicted in Fig. D2. The box plot of Xsum and CNN/DM dataset shows that the variability of attention vs. DeepLIFT and DeepLIFT vs. Gradient SHAP is high for rank agreement scores compared to all other method pairs. The variability of rank agreement scores is relatively lower in CNN/DM dataset compared to Xsum.

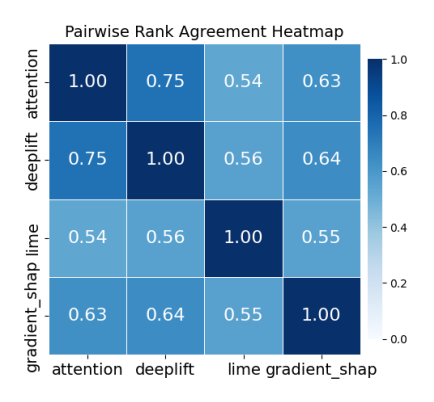


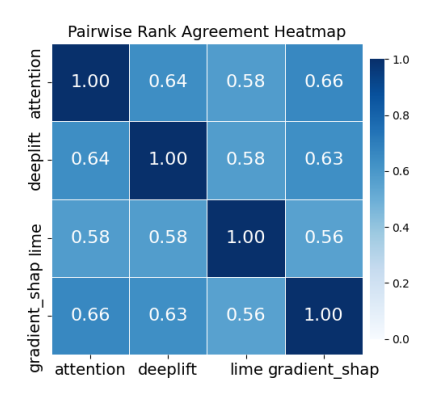


- (a) Box plot of rank agreement with highlighted k-values for Xsum.
- (b) Box plot of rank agreement with highlighted k-values for ${\rm CNN/DM}$.

Fig. D2: Box plot of Average rank agreement scores across highlighted k-values for Xsum (Fig. D2a) and CNN/DM dataset (Fig. D2b). The box plot of the Xsum and CNN/DM dataset indicates low variability of rank agreement scores.

• Pairwise Rank Agreement Heatmaps: The Fig. D3 illustrates the average pairwise rank agreement scores for both datasets. The magnitude of agreement scores based on pairwise rank agreement is relatively higher compared to the scores achieved by all other metrics.



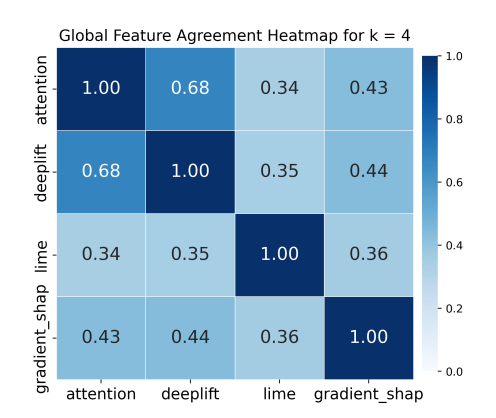


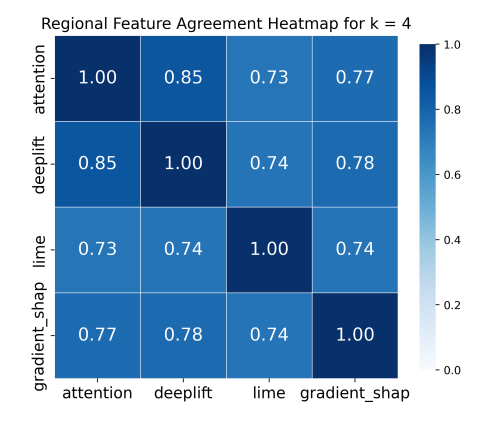
(a) Pairwise rank agreement heatmap for (b) Pairwise rank agreement heatmap for Xsum. CNN/DM.

Fig. D3: Average pairwise rank agreement heatmap for Xsum (D3a) and CNN/DM (D3b) datasets.

D.2 Disagreement analysis after applying RXAI framework (Same representative batch used in Section:4.1)

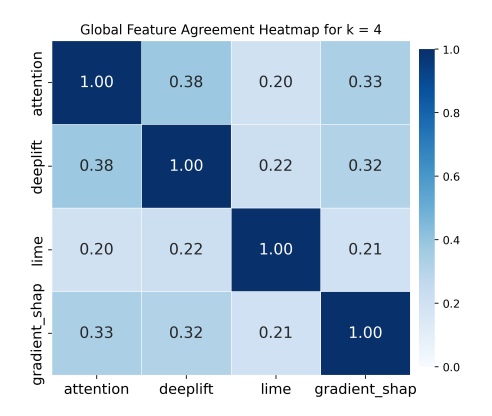
• Effectiveness of RXAI Framework: The heatmaps in Figure: D4 and Figure: D5 are added to compare the effectiveness of RXAI framework for k=4 across different XAI method pairs. The results clearly indicate enhanced feature agreement scores.

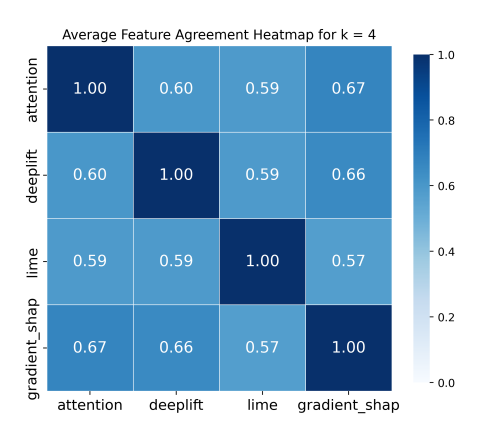




- (a) Global feature agreement heatmap for k=4 on XSum dataset.
- (b) Regional feature agreement heatmap for k=4 on XSum dataset.

Fig. D4: Global vs. Regional explanation heatmap based on feature agreement for k=4 on XSum dataset. The heatmaps demonstrate significant improvement with p-values <0.05 (refer Table: D9) across all method pairs for feature agreement scores at the regional level compared to the global analysis.

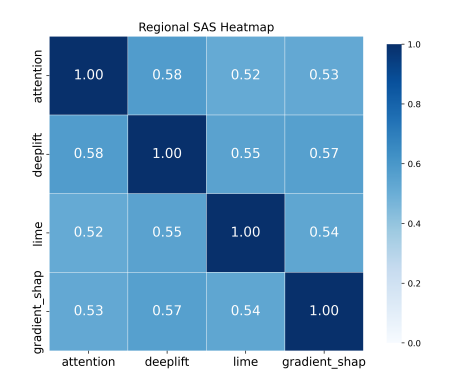


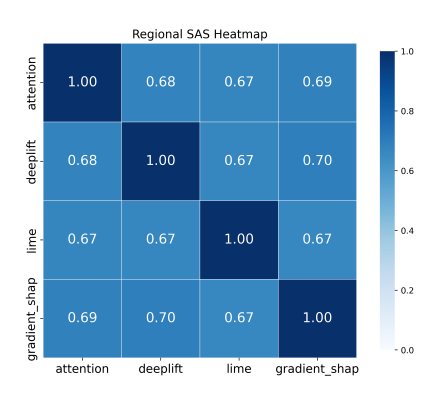


- (a) Global feature agreement for $\mathbf{k}=4$ on CNN/DM dataset.
- (b) Regional feature agreement heatmap for k=4 on CNN/DM dataset.

Fig. D5: Global vs. Regional explanation heatmap based on feature agreement for k=4 on CNN/DM dataset. The heatmaps demonstrate significant improvement with p-values <0.05 (refer Table: D10) across all method pairs for feature agreement scores at the regional level compared to the global analysis.

• Semantic Alignment Score Analysis: The impact of RXAI framework on semantic alignment is illustrated in Figure. D6. The heatmap presents average SAS scores aggregated across all k-values due to its consistent nature. The results indicates that RXAI framework does not lead to a significant improvement in semantic alignment scores.

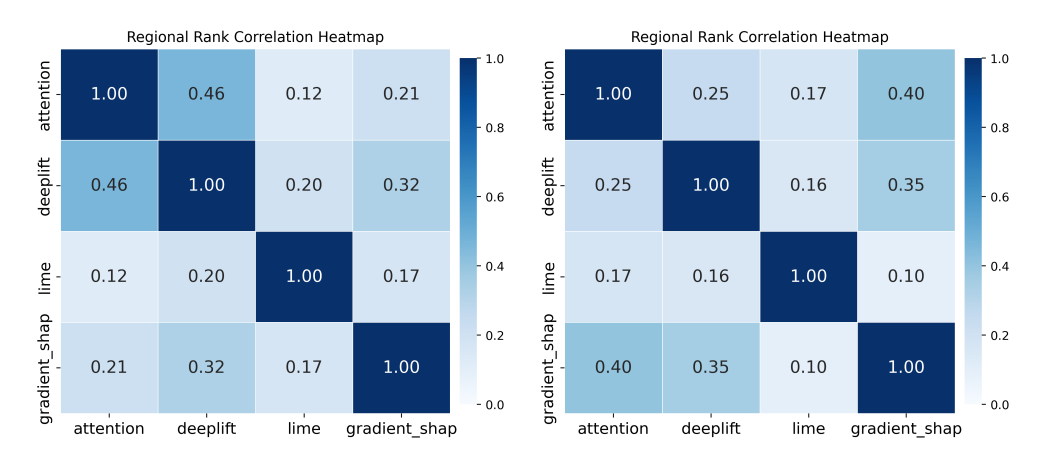




(a) SAS heatmap for segmented articles of (b) SAS heatmap for segmented articles of Xsum. CNN/DM.

Fig. D6: Average SAS heatmap of Segmented articles of Xsum (Fig. D6a) and CNN/DM D6b datasets. Overall agreement scores based on SAS indicates no significant improvement in semantic alignment scores after segmentation.

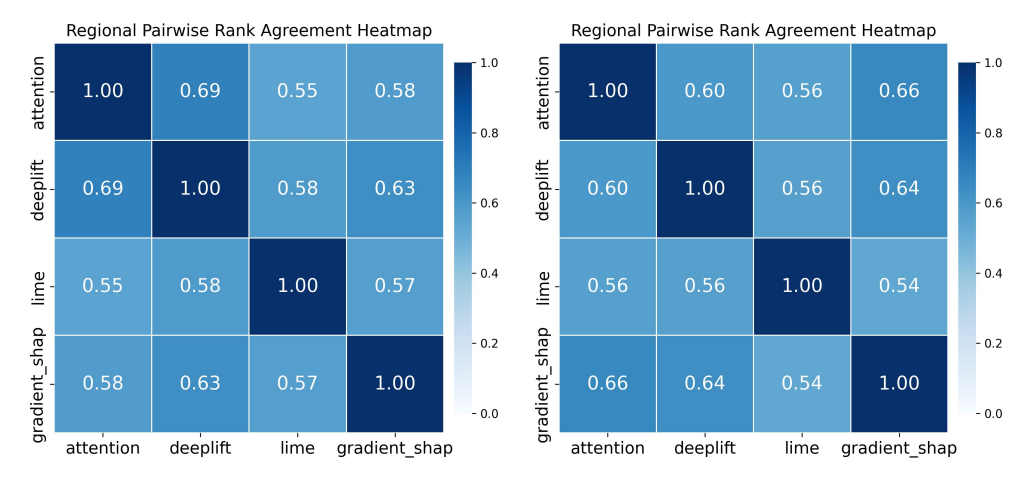
• Rank Correlation Analysis: The disagreement analysis of Regional Rank Correlation analysis shows no improvement in disagreement scores after applying the RXAI framework, as shown in Figure D7.



- (a) Rank correlation heatmap for segmented articles of Xsum.
- (b) Rank correlation heatmap for segmented articles of CNN/DM.

Fig. D7: Average spearman rank correlation heatmap of Segmented articles of Xsum (Fig. D7a) and CNN/DM D7b datasets. Overall agreement scores based on rank correlation are low, indicating no improvement in disagreement scores after segmentation.

• Pairwise Rank Agreement Analysis: The disagreement analysis of Pairwise Rank Agreement metric on Xsum and CNN/DM datasets after implementing RXAI framework is depicted in Fig. D8. The pairwise rank agreement heatmap shows a moderate degree of agreement between most methods in both datasets. Segmentation does not help in improving the pairwise rank agreement scores.



- (a) Pairwise Rank Agreement Heatmap (Segmented Articles).
- (b) Pairwise Rank Agreement Heatmap (Segmented Articles).

Fig. D8: Average pairwise rank agreement heatmap for segmented explanations of Xsum (D3a) and CNN/DM (D3b) datasets. The heatmap of both datasets highlights that segmentation does not help in enhancing the pairwise rank agreement scores and mostly stays consistent with the global pairwise rank agreement score.

D.3 Batched Analysis of XAI Disagreement

D.3.1 Global Disagreement Analysis

The disagreement analysis was carried out across 11 random batches, each with 500 samples (5500 total), to guarantee statistically robust results. While results from one representative batch are included in the main results Section: 4.1, this appendix presents findings from an additional representative batch along with average agreement scores across all 11 batches. The results from this batch, discussed in this section, demonstrate strong consistency in agreement scores across XAI methods. Notably, this consistency is not limited to these two batches. To evaluate whether the observed consistency persists across all batches, we employed a one-way ANOVA test, the results of which are discussed in Section D.3.3. Here, we present batch-level agreement comparisons (Batch 2 from the XSum and CNN/DM dataset) across four key metrics: SAS, Feature Agreement, and Spearman Rank Correlation.

To evaluate the degree of disagreement of an individual explanation method with every other XAI method, we conducted combined comparisons at k=4. We measured how well each XAI method agrees with every other method by averaging pairwise feature agreement scores. This approach enables us to determine the consistency or divergence of a given method related to the rest, offering a combined perspective on the consistency of XAI methods. The results show that attention vs all other methods attained the FA value of 0.49, followed by DeepLIFT vs all other methods having FA

value of 0.5, followed by Gradient SHAP vs all other methods having FA value of 0.43 and LIME vs all other methods having the lowest FA value of 0.38.

A summarized view of global disagreement analysis based on Feature agreement and Rank agreement across all 11 batches is presented in Table D4 and Table D5. The results of feature and Rank agreement at k=4 and k=8 with very low standard deviation values indicate that the global agreement scores remain highly consistent across batches.

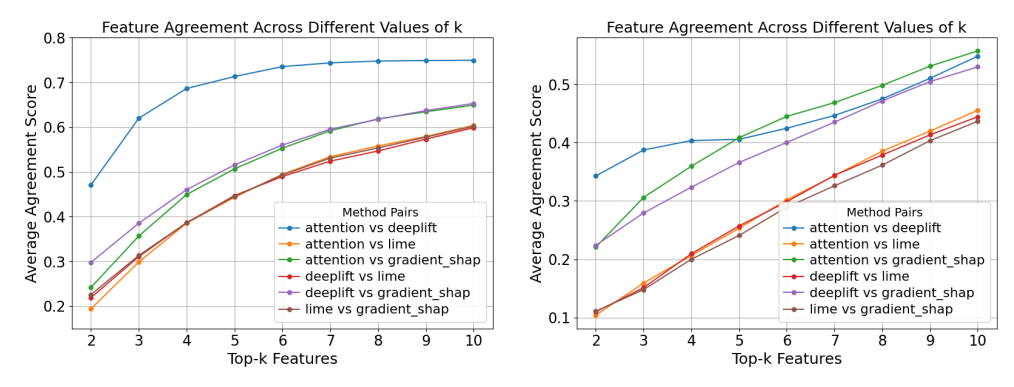
Table D4: Mean Feature Agreement (FA) across 11 batches for XSum and CNN/DM datasets, computed for selected k values. The table highlights average agreement consistency with low standard deviation values, indicating consistent FA values for k=4 and k=8.

Method Pair	XSum $k = 4$	XSum $k = 8$	CNN $k=4$	$\mathbf{CNN} \ k = 8$
Attention vs DeepLIFT	0.68 ± 0.007	0.75 ± 0.006	0.40 ± 0.018	0.55 ± 0.026
Attention vs Gradient SHAP	0.44 ± 0.017	0.62 ± 0.007	0.34 ± 0.013	0.54 ± 0.015
Attention vs LIME	0.36 ± 0.014	0.55 ± 0.011	0.23 ± 0.018	0.44 ± 0.031
DeepLIFT vs Gradient SHAP	0.45 ± 0.011	0.62 ± 0.009	0.34 ± 0.019	0.52 ± 0.023
DeepLIFT vs LIME	0.37 ± 0.017	0.55 ± 0.011	0.24 ± 0.015	0.44 ± 0.029
LIME vs Gradient SHAP	0.38 ± 0.011	0.56 ± 0.010	0.23 ± 0.018	0.42 ± 0.033

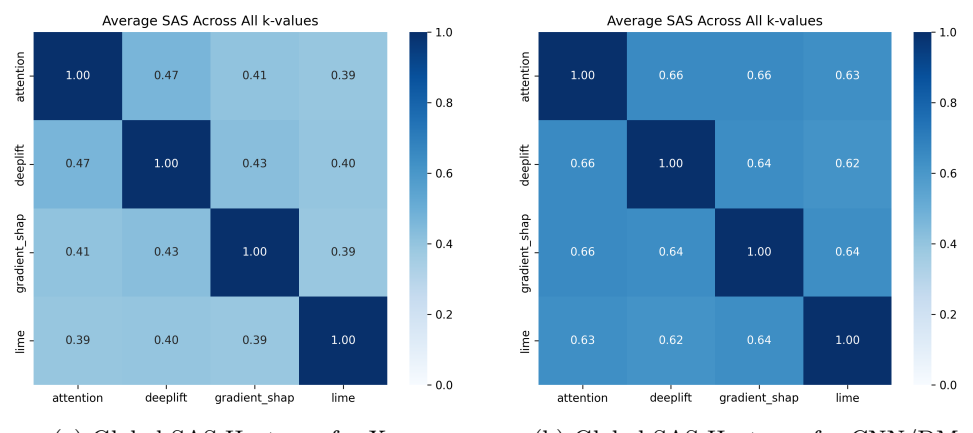
Table D5: Mean Rank Agreement (RA) across 11 batches for XSum and CNN/DM datasets, computed for selected k values. The table highlights average agreement consistency with low standard deviation values, indicating consistency for k=4 and k=8.

Method Pair	XSum $k = 4$	XSum $k = 8$	CNN $k=4$	$\mathbf{CNN}\ k = 8$
Attention vs DeepLIFT	0.19 ± 0.005	0.15 ± 0.004	0.12 ± 0.010	0.09 ± 0.006
Attention vs Gradient SHAP	0.12 ± 0.012	0.10 ± 0.006	0.08 ± 0.009	0.07 ± 0.006
Attention vs LIME	0.10 ± 0.005	0.08 ± 0.003	0.06 ± 0.007	0.06 ± 0.006
DeepLIFT vs Gradient SHAP	0.13 ± 0.009	0.11 ± 0.005	0.10 ± 0.009	0.08 ± 0.006
DeepLIFT vs LIME	0.10 ± 0.009	0.08 ± 0.004	0.06 ± 0.004	0.06 ± 0.005
LIME vs Gradient SHAP	0.10 ± 0.008	0.09 ± 0.005	0.06 ± 0.006	0.05 ± 0.005

The results from Batch 2 presented in figures: D9, D10, D11 illustrate similar agreement patterns between explanation methods as discussed in section: 4.1. While slight variations are observed, the scores across batches do not vary significantly. This consistency across all 11 batches supports the robustness of our findings reported in the main results section.

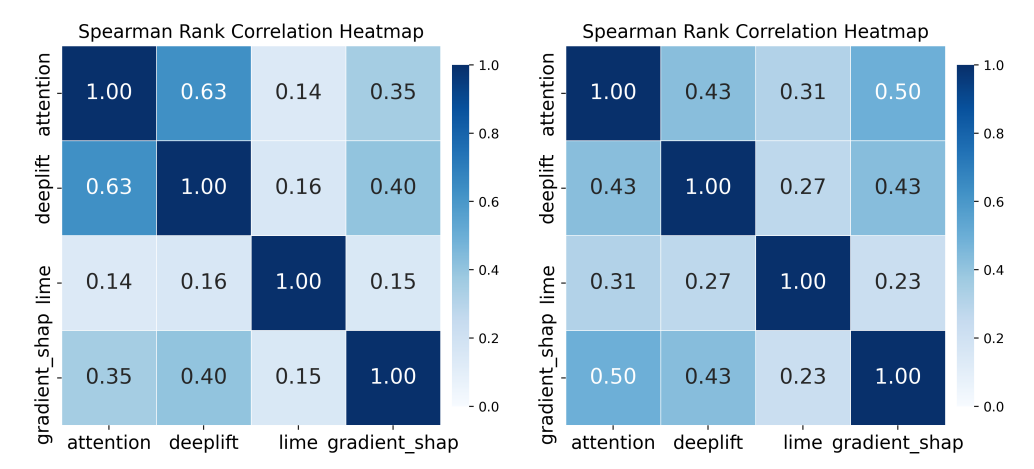


- (a) Global Feature Agreement scores for (b) Global Feature Agreement scores for Xsum dataset across different k-values.
- **Fig. D9**: Global Feature Agreement across different top-k values on XSum and CNN/DM datasets. The trend of global feature agreement scores across different method pairs is similar to the previous sample set analyzed in main results section 4.1.



- (a) Global SAS Heatmap for Xsum.
- (b) Global SAS Heatmap for CNN/DM.

Fig. D10: Global Semantic Alignment Score (SAS) heatmaps for XSum and CNN/DM datasets across all k-values. The scores of global semantic alignment for this batch is consistent and depicts similar trend as other batches.



- (a) Global Spearman Rank Correlation Heatmap for Xsum dataset
- (b) Global Spearman Rank Correlation for CNN/Dailymail dataset

Fig. D11: Global Spearman Rank Correlation analysis across XAI methods on XSum and CNN/DM dataset. The heatmap depicts similar trends as observed in the previous sample set of global rank correlation analysis.

D.3.2 Regional Disagreement Analysis:

We also evaluated the consistency of RXAI scores across batches; however, the agreement scores after segmentation exhibited slight variations among batches, which may be attributed to variation of segment lengths across batches. The summarized view of the RXAI framework based on Feature and Rank agreement across all 11 batches is presented in Table D6 and Table D7.

Table D6: Mean Feature Agreement (FA) across 11 batches for XSum and CNN/DM datasets, computed for selected k values. The table highlights Regional average feature agreement consistency with low standard deviation values.

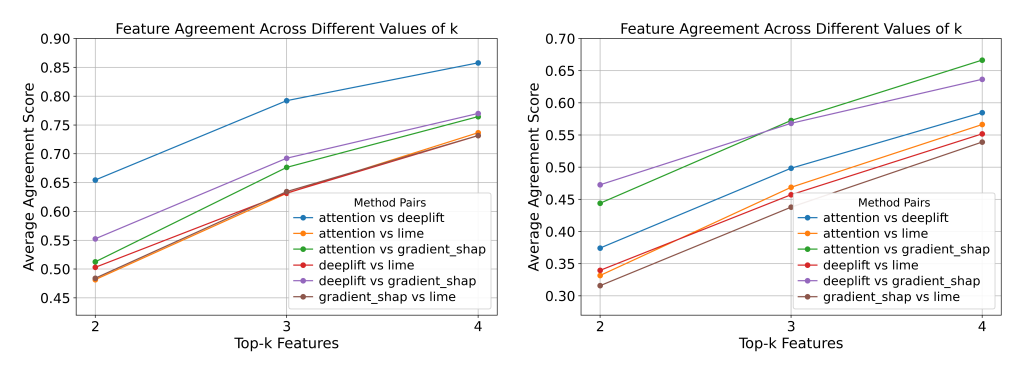
Method Pair	XSum $k = 2$	XSum $k = 4$	$\mathbf{CNN} \ k = 2$	$\mathbf{CNN} \ k = 4$
attention vs DeepLIFT	0.61 ± 0.050	0.82 ± 0.049	0.39 ± 0.037	0.65 ± 0.058
attention vs Gradient_SHAP	0.44 ± 0.092	0.69 ± 0.103	0.45 ± 0.035	0.71 ± 0.052
attention vs lime	0.41 ± 0.093	0.64 ± 0.116	0.36 ± 0.039	0.63 ± 0.063
DeepLIFT vs Gradient_SHAP	0.49 ± 0.096	0.70 ± 0.105	0.48 ± 0.032	0.69 ± 0.054
DeepLIFT vs lime	0.43 ± 0.094	0.65 ± 0.113	0.35 ± 0.037	0.63 ± 0.068
lime vs gradient_ $SHAP$	0.42 ± 0.093	0.65 ± 0.118	0.34 ± 0.038	0.62 ± 0.067

To assess the effectiveness of the RXAI framework and how consistent it is in enhancing agreement between XAI methods, we have added the RXAI analysis on batch 2 below. Here, we present batch-level regional agreement comparisons (Batch

Table D7: Mean Rank Agreement (RA) scores for XSum and CNN datasets, computed for selected k values. The table highlights Regional average agreement consistency with low standard deviation values.

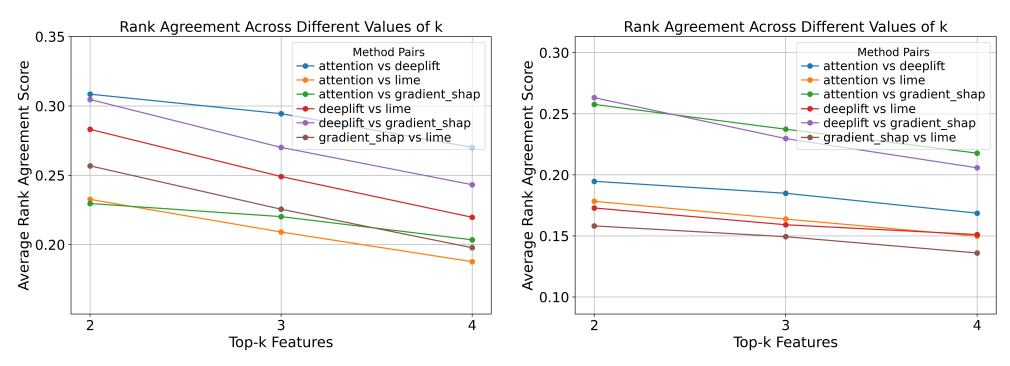
Method Pair	XSum $k=2$	XSum $k = 4$	CNN $k=2$	CNN $k=4$
attention vs DeepLIFT	0.29 ± 0.030	0.25 ± 0.021	0.19 ± 0.020	0.18 ± 0.021
attention vs Gradient_SHAP	0.21 ± 0.038	0.19 ± 0.028	0.23 ± 0.021	0.22 ± 0.018
attention vs lime	0.21 ± 0.045	0.17 ± 0.032	0.17 ± 0.022	0.16 ± 0.018
DeepLIFT vs gradient_SHAP	0.28 ± 0.052	0.23 ± 0.037	0.28 ± 0.021	0.22 ± 0.021
DeepLIFT vs lime	0.25 ± 0.052	0.20 ± 0.032	0.17 ± 0.015	0.16 ± 0.015
lime vs gradient_SHAP	0.23 ± 0.048	0.19 ± 0.033	0.17 ± 0.021	0.15 ± 0.020

2 from the XSum and CNN/DM dataset) across four key metrics: SAS, Spearman Rank Correlation, Feature Agreement, and Rank Agreement. The results of the RXAI approach on Batch 2, presented in figures: D12, D13, D14 and D15 illustrate similar agreement enhancement patterns between XAI methods as observed in section: 4.1. While the variations are observed between the enhanced agreement scores, they vary with a low standard deviation value as highlighted in Table D6 and Table D7. This consistency of improvement across all 11 batches supports the hypothesis and robustness of our findings reported in the main results section.



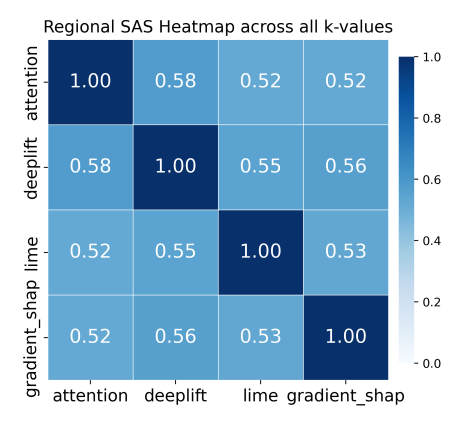
- (a) Feature Agreement Line-plot for Xsum dataset(segmented articles)
- (b) Feature Agreement Line-plot for CNN/DM dataset(segmented articles)

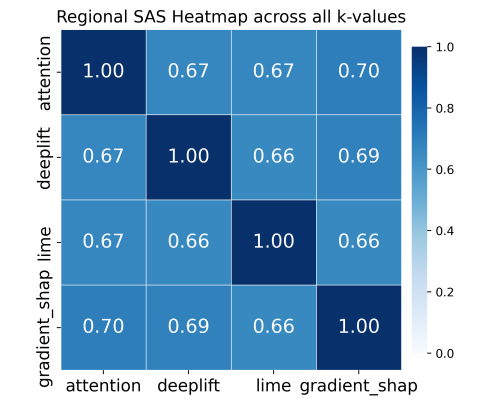
Fig. D12: Average Feature Agreement Line-plots on XSum and CNN/DM datasets after Segmentation. The Line plot depicts similar trends as observed in the previous sample set of segmented articles.



- (a) Rank Agreement Line-plot for Xsum dataset (segmented articles) $\,$
- (b) Rank Agreement Line-plot for CNN/DM dataset(segmented articles)

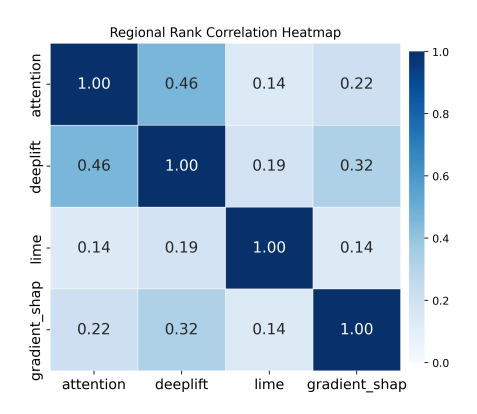
Fig. D13: Average Rank Agreement Line-plots on XSum and CNN/DM datasets after Segmentation. The Line plot depicts similar trends as observed in the previous sample set of segmented articles.

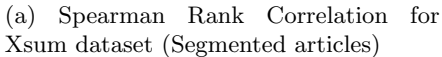


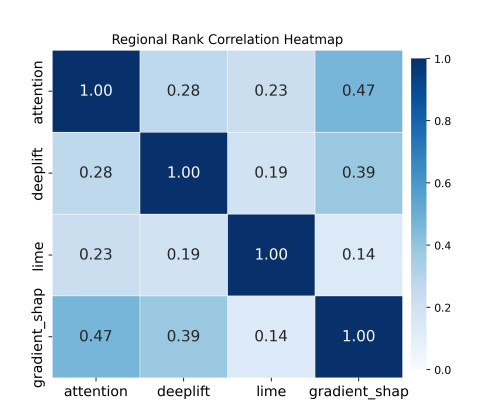


- (a) Regional XSum Semantic Alignment score across k values (Segmented articles)
- (b) Regional CNN/DM Semantic Alignment Score across k values (Segmented articles)

Fig. D14: SAS across XAI methods on XSum and CNN datasets after Segmentation. The trend of SAS scores is the same as the previously analyzed sample.







(b) Spearman Rank Correlation for CNN/DM dataset (Segmented articles)

Fig. D15: Spearman Rank Correlation across XAI methods on XSum and CNN datasets after segmentation. The results of Spearman Rank Agreement in this batch are also consistent.

D.3.3 Statistical Test Results and analysis

1. One-way ANOVA:

(a) Conducting ANOVA on Global Disagreement Results:

This test was used to determine whether the mean global agreement scores (Feature Agreement and Rank Agreement) significantly differ across 11 independently sampled batches. The test was conducted for each method pair and top-k value ($k \in \{2, ..., 10\}$), resulting in 54 tests per agreement type. As shown in Table D8, the XSum dataset showed relatively stable behavior across batches, with only 6% of FA tests and 6% of RA tests found to be significant (p < 0.05). In contrast, the CNN dataset exhibited high batch sensitivity in FA scores (88.9% significant) and moderate variation in RA scores (42.6% significant).

- (b) Conducting ANOVA on Local Disagreement Results: The same test was executed across all 11 batches of Regional agreement analysis scores. The RXAI framework helps in improving agreement; however, the magnitude of improvement varies across batches for both Xsum and CNN/DM datasets. Hence, the p-values across batches of RXAI analysis were below 0.05, indicating that the agreement scores are not consistent across batches after applying RXAI, which may be attributed to segment length across batches. However, the analysis done in table D7 and D6 shows a very low value of variance across the mean score of agreement for all batches.
- 2. Wilcoxon Signed-Rank Test: To evaluate the impact of RXAI approach on agreement between XAI methods, we applied the Wilcoxon signed-rank test, a non-parametric test for paired data. We compared agreement scores before (global) and after segmentation (regional) for each article, across method pairs and $k \in \{2, 3, 4\}$, over 11 batches. The results show strong improvements. For the XSum dataset,

Table D8: One-way ANOVA summary for global agreement score consistency across 11 batches.

Dataset	Agreement	Significant	Not-Significant	% Not Significant
XSum	Feature Agreement (FA)	3	51	94%
XSum	Rank Agreement (RA)	3	51	94%
CNN	Feature Agreement (FA)	48	6	11.0%
CNN	Rank Agreement (RA)	23	31	57.6%

 ${\sim}99\%$ of Feature Agreement (FA) and ${\sim}83\%$ of Rank Agreement (RA) comparisons across 11 batches showed statistically significant improvement (p<0.05 with very low p-values). Similarly for CNN/DM dataset approximately ${\sim}97\%$ of FA and ${\sim}85\%$ of RA comparisons across all batches showed significant improvement. These results confirms the effectiveness of RXAI approach, which helps in enhancing explanation consistency. Table: D9 and D10 shows sample results of p-values.

Table D9: Wilcoxon signed-rank test p-values for Feature Agreement values across Xsum dataset's representative batch of 500 samples discussed in section 4.1. The p-values clearly indicate that there is a significant difference between agreement scores before and after segmentation for each method pair at different k-values, supporting our hypothesis.

Method Pair	k = 2	k = 3	k = 4
attention vs DeepLIFT	7.751×10^{-20}	2.156×10^{-29} 1.547×10^{-54} 2.131×10^{-47} 2.456×10^{-56} 1.713×10^{-49} 2.384×10^{-52}	1.622×10^{-43}
attention vs lime	2.586×10^{-42}		1.610×10^{-66}
attention vs Gradient_SHAP	2.287×10^{-38}		5.710×10^{-61}
DeepLIFT vs lime	1.858×10^{-42}		1.942×10^{-65}
DeepLIFT vs Gradient_SHAP	1.662×10^{-36}		6.463×10^{-61}
lime vs Gradient_SHAP	8.405×10^{-41}		1.052×10^{-64}

Table D10: Wilcoxon signed-rank test *p*-values for FA values across CNN/DM dataset's representative batch of 500 samples discussed in section 4.1. The p-values clearly indicate that there is a significant difference between agreement scores before and after segmentation for each method pair at different k-values, supporting our hypothesis.

Method Pair	k = 2	k = 3	k = 4
attention vs DeepLIFT	5.185×10^{-1}	1.370×10^{-7}	1.312×10^{-25}
attention vs lime	6.122×10^{-37}	1.441×10^{-65}	4.503×10^{-76}
attention vs Gradient_SHAP	1.990×10^{-27}	2.399×10^{-50}	3.426×10^{-71}
DeepLIFT vs lime	5.400×10^{-37}	3.888×10^{-65}	2.578×10^{-74}
DeepLIFT vs Gradient_SHAP	1.510×10^{-37}	1.699×10^{-57}	8.874×10^{-72}
lime vs Gradient_SHAP	1.631×10^{-33}	7.157×10^{-66}	1.634×10^{-74}

D.3.4 Impact of RXAI Framework:

From the empirical analysis and the statistical test results it is evident that RXAI framework helps in mitigating the disagreement problem. However, the framework relies on clustering the text data in meaningful, coherent segments using k-means clustering, which may introduce semantic or coherence drift between input articles and segments. To assess this, we have conducted an analysis in two steps:

1. Comparing semantic similarity between input articles and their segmented version across both datasets: Table D11 illustrates the semantic similarity results on two representative samples of Xsum and CNN/DM datasets. The similarity is measured between the Input article and the segmented article (concatenated), as well as the input article with individual segments. The global similarity score with the concatenated segment text remains high (≥0.90) for both datasets. The segmentwise score is, however, slightly lower than the concatenated score. This analysis confirms that segmentation largely preserves the meaning of the article, validating the reliability of the RXAI framework.

Table D11: Semantic similarity between original articles and segmented versions across two batches from XSum and CNN/DM datasets. Global similarity is computed using concatenated segments; segment-wise reflects the average of individual segment similarities.

Metric	XSum Batch-1	XSum Batch-2	CNN Batch-1	CNN Batch-2
Avg Segment-wise Similarity	0.77 ± 0.10	0.80 ± 0.10	0.76 ± 0.08	0.75 ± 0.01
Global Semantic Similarity (Concatenated)	0.94 ± 0.07	0.97 ± 0.06	0.90 ± 0.08	0.92 ± 0.08

2. The Second step is to compare the Coherence score of the article and its segmented version across both datasets. To verify coherence drift, we utilized the Coherence Momentum model from SGNLP (Jwalapuram, Joty, & Lin, 2022). This neural model employs a momentum encoder and hard negative mining during training to assess coherence. Given a piece of text, it outputs a coherence score, which is meaningful only in comparative settings. The text with the higher score is considered more coherent. In our study, we use this model to compare coherence between the original article and its segmented version. The coherence score of each input article and segmented article is calculated, along with the drift between the two scores. The average coherence value for the full article vs. the Segmented article is computed to analyze coherence preservation. In some cases, the coherence score of segmented articles is higher than the full article.

The results of coherence analysis are depicted in Table D12. From the overall average coherence scores of Input articles vs segmented articles as well as the drift score highlights that the segmentation does introduce coherence drift; however, the drift is moderate, ranging from 4.8 to 8.1, with low standard deviation values. Overall, these results highlight that while RXAI introduces moderate coherence

drift, it largely preserves the semantic structure and coherence between the input article and the segmented article.

(a) Coherence analysis of XSum dataset across two batches

Metric	Batch-1	Batch-2
Coherence Full (Mean) Coherence Segmented (Mean) Drift (Mean)	-9.499 -15.763 6.264	-8.223 -13.477 5.255
Coherence Full (Std Dev) Coherence Segmented (Std Dev) Drift (Std Dev)	9.356 8.378 6.279	8.645 8.386 7.450

(b) Coherence analysis of CNN/DM dataset across two batches

Metric	Batch-1	Batch-2
Coherence Full (Mean) Coherence Segmented (Mean) Drift (Mean)	-8.542 -13.365 4.822	-9.360 -17.466 8.106
Coherence Full (Std Dev) Coherence Segmented (Std Dev) Drift (Std Dev)	8.148 7.709 6.848	8.769 7.289 7.083

Table D12: Coherence scores and drift for XSum and CNN/DM datasets across two batches. Coherence Full refers to the original article, Coherence Segmented to the segmented version, and Drift is their absolute difference.

Appendix E JavaScript Visualization tool

The JavaScript visualization tool features a user-friendly interface for inputting text, attribution scores, and summaries. Fig. E16 showcases the tool's interface, which accepts source sentences and their corresponding normalized attribution scores, allowing users to explore the influence of each sentence on the summary generation.

Let's Understand Your Text Summarization Model

Select Top N Sentences: All Sentences >	
Title:	
Summary:	
Input Sentences (Enclosed in quotation and Separated by commas):	
Weights (Comma-separated):	
Generate Text Plot	

Fig. E16: JavaScript tool interface along with the input fields